Summer 7-17-2017

Assessing the utility of phenylene ethynylenes against Candida species pathogens

Rina Sylejmani
University of New Mexico

Rina Sylejmani
Candidate

Biomedical Engineering
Department

This thesis is approved, and it is acceptable in quality and form for publication:

Approved by the Thesis Committee:

Aaron K. Neumann , Chairperson

David G. Whitten

Eva Y. Chi

Assessing the utility of phenylene ethynylenes against *Candida* species pathogens

By

Rina Sylejmani

B.S. Chemistry, University of New Mexico, 2015
B.S. Biology, University of New Mexico, 2015

THESIS

Submitted in Partial Fulfillment of the
Requirements for the Degree of

Master of Science
Biomedical Engineering

The University of New Mexico
Albuquerque, NM

July 2017

DEDICATION

This thesis is dedicated to my family, especially my dad,
the first and best engineer I know.

ACKNOWLEDGMENTS

I take great pride and gratitude in being part of the Neumann Research Group throughout the duration of my graduate studies. I want to express many thanks to my graduate advisor and chair, Dr. Aaron Neumann, for continuously showing me what it means to practice sound science. From his countless advice and ideas, he has been the epitome of a great scientist, and I hope to emulate the same passion he brings to his work in my future endeavors. I would like to extend my appreciation to the members of my committee of studies: Dr. David Whitten and Dr. Eva Chi. Their continuous guidance has been fundamental in the completion of my project and I will always remember their invaluable support. I would also like to thank Dr. Thomas Howdieshell for his input throughout the duration of this project.

Additionally, I want to thank Dr. Harry Pappas for his unwavering mentorship. Thank you to all the members of the Neumann lab for their assistance. I want to to give a special thanks to Carmen Martinez and Eddy Anaya, for their friendship, help and stimulating discussion when the science did not cooperate. I am grateful to the University of New Mexico for the opportunities and resources they have provided me to improve scholastically. I want to thank the numerous friends I have made as part of this program for always being willing to troubleshot and teach me new methods – Adrian Luna, Jason Joyner, Sebastian Restrepo Cruz, and Florencia Monge.

Lastly, when it comes to acknowledging those that are most instrumental to my success, my family deserves insurmountable thanks. As war refugees, my parents have made great sacrifices and taught me to value my education. My siblings – Gresa, Dijar and Donart have been the best support system. They provide relentless laughs and advice in the most stressful of times and their kindness will always be cherished.

Assessing the utility of phenylene ethynylenes against *Candida* species pathogens

By

Rina Sylejmani

B.S. Chemistry, University of New Mexico, 2015
B.S. Biology, University of New Mexico, 2015
M.S. Biomedical Engineering, University of New Mexico, 2017

ABSTRACT

Candida species are the cause of many bloodstream infections through contamination of indwelling medical devices. These infections account for a 40% mortality rate, posing a significant risk to immunocompromised patients. Traditional treatments against *Candida* infections include amphotericin B and various azole treatments. Unfortunately, these treatments are associated with high toxicity, and resistant strains have become more prevalent. As a new frontier, light-activated phenylene ethynylenes have shown promising biocidal activity against Gram-positive and -negative bacterial pathogens, as well as the environmental yeast, *Saccharomyces cerevisiae*. In this thesis, we monitored the viability of *Candida* species after treatment with a cationic conjugated polymer (PPE) or oligomer (OPE) by flow cytometry in order to explore the antifungal properties of these compounds. The oligomer was found to disrupt *Candida albicans* yeast membrane integrity independent of light-activation, while the PPE is only able to do so in the presence of light, allowing for some control as to the manner which cytotoxic effects are exhibited. Furthermore, treatment with PPE-DABCO unmasked *Candida albicans* β-glucan, and increased phagocytosis by Dectin-1-expressing HEK-293 cells. Additionally OPE exhibited potent antifungal activity against *Candida albicans* and *Candida parapsilosis*, two medically significant fungal pathogens. In contrast, another major *Candida* species

pathogen, *Candida glabrata*, displayed intrinsically low susceptibility to OPE, relative to *C. ablicans* and *C. parapsilosi*s. In C. *glabrata*, the primary mechanism of azole-resistance is attributed to alterations in the ERG11 gene and over-expression of the CgCDR1 efflux pump gene. We hypothesize that similar mechanisms may account for *C. glabrata* resistance to OPE. We monitored the susceptibility of *C. glabrata* to OPE by flow cytometry after treatment with clorgyline, a broad spectrum efflux pump inhibitor. Clorgyline showed synergy with OPE in type strain ATCC2001. In summary, cationic phenylene ethynylenes show promising biocidal activity against pathogenic *Candida* spp. alone and in combination with clorgyline.

TABLE OF CONTENTS

Chapter 1 – Introduction 1

1.1 – Significance 1

1.2 – Poly(phenylene ethynylene) 1

1.3 – Drug resistance in *Candida glabrata* 3

References 4

Chapter 2 – The Antifungal Properties of Cationic p-Phenylene Ethynylenes and their Impact on β-Glucan Exposure 7

2.1 – Introduction 7

2.2 – Materials and Methods 10

2.3 – Results 15

2.4 – Discussion 27

References 32

Chapter 3 – Oligo-phenylene Ethynylene (OPE) Resistance in *Candida glabrata* 38

3.1 – Introduction 38

3.2 – Materials and Methods 38

3.3 – Results 42

3.4 – Discussion 53

References 56

Chapter 4 – Conclusions and Recommendations for Future Work 59

4.1 – Efficacy of PPE-DABCO and EO-OPE-DABCO against *Candida* spp. hyphae and biofilms 59

4.2 – Determining efflux pumps involved in OPE-resistance in *Candida glabrata* 60

4.3 – Investigating clorgyline's mechanism of action in *Candida glabrata* 61

4.4 – Potential applications of phenylene ethynylenes 61

References 63

Chapter 1

Introduction

1.1 Significance

In modern medicine, systemic candidiasis remains a pertinent healthcare problem. While immunocompromised patients are most at risk for these infections; increased microbial access to the bloodstream in burn victims and during invasive surgical procedures pose subsequent risk to immune competent patients. Annually, the United States spends millions of health care dollars in the diagnosis and treatment of these infections (1, 2) More importantly, bloodstream infections cause ~ 31,000 mortalities yearly. *Candida species* are the fourth leading cause of all bloodstream infections and account for a 40% mortality rate (1, 3, 4). The most commonly isolated species of infection is *C. albicans*, but the prevalence of other species such as *C. parapsilosis* and *C. glabrata* is increasing (5–7) . Present antifungal treatment to combat these infections include azoles, echinocandins, and polyenes. However, these traditional treatments are often associated with the rise of resistant strains and cytotoxic effects (8, 9) . The high morbidity and mortality rates associated with systemic candidiasis elicit an urgent demand for novel antifungal therapies.

1.2 Poly(phenylene ethynylene)

Light-activated poly(phenylene ethynylenes) (PPEs) have shown promising biocidal activity against Gram-positive and -negative bacterial pathogens, as well as the environmental yeast, *Saccharomyces cerevisiae* (10–14) . In addition to their promising antimicrobial activity, they exhibit low toxicity to human cells in vitro (15). The purpose of

this thesis aims to test the utility of these compounds against a range of *Candida* species pathogens and assess the potential for resistance. The experiments described explored the antimicrobial activity of two particular phenylene ethynylene compounds, PPE-DABCO and EO-PPE-DABCO. The antimicrobial activity of poly(phenylene ethynylene) compounds such as PPE-DABCO and EO-PPE-DABCO can be attributed to several intrinsic characteristics. The chemical structure of these compounds renders them capable of inducing broad-spectrum cell damage. The phenylene ethynylenes studied consist of alternating phenyl and acetylenic groups with appended cationic groups (Fig. 1).

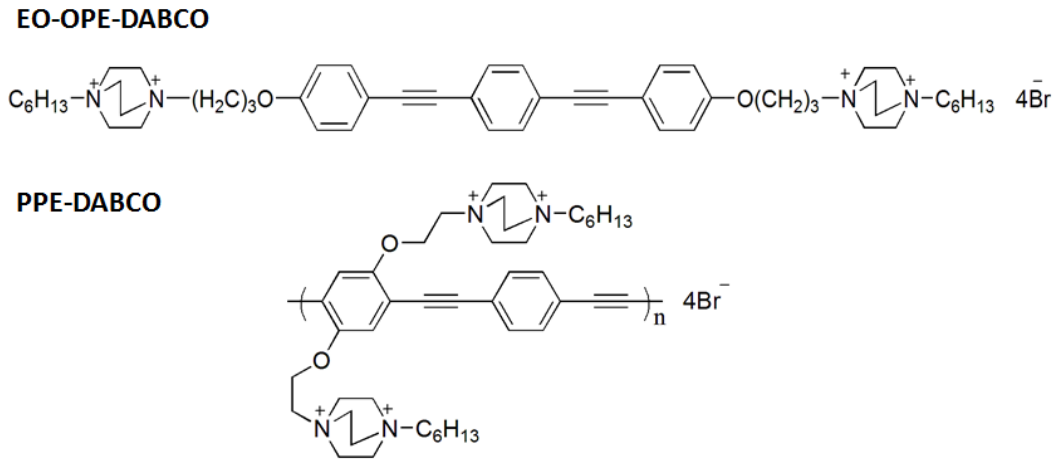

Figure 1: Molecular structures of oligomeric EO-OPE-DABCO (top) and polymeric PPE-DABCO (bottom).

The interaction of the cationic quaternary ammonium groups with net-anionic membranes and cell walls facilitates interactions with microbes, leading to membrane perturbation,

pore formation, and the leakage of cell contents (16). In addition, when PEs are irradiated by the appropriate wavelength, the backbone produces reactive oxygen species (ROS) that induce rapid cell death (17, 18).

1.3 Drug resistance in *Candida glabrata*

While *C. ablicans* is most commonly isolated species of bloodstream and mucosal candidiasis, *C.glabrata* poses a significant threat because of its intrinsic resistance to the commonly prescribed antifungal known as fluconazole (19, 20). Fluconazole targets the ergosterol biosynthetic pathway in fungi. *C. glabrata* is not only intrinsically resistant to fluconazole but resistance has been observed to increase during treatment (21, 22). The reduced efficacy of fluconazole against *C. glabrata* has been largely attributed to alternations in the target enzyme, ERG11, consequently reducing the effect of the drug. Additionally drug resistance is mediated by drug efflux pumps, specifically, the increased expression of ABC transporters known as CgCdr1, CgCdr2 (Pdh1), and CgSnq2 (23, 24). These transporters serve to transport substances across the membrane and are found primarily in the plasma membrane and also in the membranes of organelles . In *C. glabrata,* overexpression of proteins that pump drug out the cell has been correlated with high-level azole resistance (25, 26) . Animal studies have shown that strains with hyperactive *C. glabrata* PDR1 (CgPDR1) alleles that upregulate CgCDR1, CgCDR2,and CgSNQ2 expression were more virulent in mice than strains with wild-type alleles (27). The testing of new antifungals against *C. glabrata* requires careful consideration in overcoming efflux mediated drug resistance.

References

1. Wenzel RP, Edmond MB. 2001. The impact of hospital-acquired bloodstream infections. Emerg Infect Dis 7:174–177.
2. Anderson DJ, Kirkland KB, Kaye KS, Thacker II PA, Kanafani ZA, Auten G, Sexton DJ. 2007. Underresourced Hospital Infection Control and Prevention Programs: Penny Wise, Pound Foolish? • . Infect Control Hosp Epidemiol 28:767–773.
3. Edmond MB, Wallace SE, McClish DK, Pfaller MA, Jones RN, Wenzel RP. 1999. Nosocomial bloodstream infections in United States hospitals: A three-year analysis. Clin Infect Dis 29:239–244.
4. Wisplinghoff H, Bischoff T, Tallent SM, Seifert H, Wenzel RP, Edmond MB. 2004. Nosocomial bloodstream infections in US hospitals: analysis of 24,179 cases from a prospective nationwide surveillance study. Clin Infect Dis 39:309–317.
5. Ellis ME, Al-Abdely H, Sandridge a, Greer W, Ventura W. 2001. Fungal endocarditis: evidence in the world literature, 1965-1995. Clin Infect Dis 32:50–62.
6. Wingard JR. 1995. Importance of Candida Species Other Than Candida-Albicans as Pathogens in Oncology Patients. Clin Infect Dis 20:115–125.
7. Keynan Y, Rubinstein E. 2007. Fungal endocarditis. Curr Fungal Infect Rep 1:25–32.
8. Castanheira, Mariana, Messer, Shawn A., Rhomberg, Paul R., Pfaller MA. 2016. ntifungal susceptibility patterns of a global collection of fungal isolates: results of the SENTRY Antifungal Surveillance Program. Diagn Microbiol Infect Dis 85:200–204.
9. CDC. 2013. ntibiotic resistance threats in the United States. US Dep Heal Hum Serv.
10. Wang Y, Chi EY, Natvig DO, Schanze KS, Whitten DG. 2013. Antimicrobial activity of cationic conjugated polyelectrolytes and oligomers against Saccharomyces cerevisiae vegetative cells and ascospores. ACS Appl Mater Interfaces 5:4555–61.
11. Lu L, Rininsland FH, Wittenburg SK, Achyuthan KE, McBranch DW, Whitten DG. 2005. Biocidal activity of a light-absorbing fluorescent conjugated polyelectrolyte. Langmuir 21:10154–10159.
12. Corbitt TS, Sommer JR, Chemburu S, Ogawa K, Ista LK, Lopez GP, Whitten DG, Schanze KS. 2009. Conjugated polyelectrolyte capsules: Light-activated antimicrobial micro “roach Motels.” ACS Appl Mater Interfaces 1:48–52.

13. Chemburu S, Corbitt TS, Ista LK, Ji E, Fulghum J, Lopez GP, Ogawa K, Schanze KS, Whitten DG. 2008. Light-induced biocidal action of conjugated polyelectrolytes supported on colloids. Langmuir 24:11053–11062.

14. Wang Y, Canady TD, Zhou Z, Tang Y, Price DN, Bear DG, Chi EY, Schanze KS, Whitten DG. 2011. Cationic phenylene ethynylene polymers and oligomers exhibit efficient antiviral activity. ACS Appl Mater Interfaces 3:2209–2214.

15. Wilde KN, Whitten DG, Canavan HE. 2013. In vitro cytotoxicity of antimicrobial conjugated electrolytes: Interactions with mammalian cells. ACS Appl Mater Interfaces 5:9305–9311.

16. Wang Y, Jones EM, Tang Y, Ji E, Lopez GP, Chi EY, Schanze KS, Whitten DG. 2011. Effect of Polymer Chain Length on Membrane Perturbation Activity of Cationic Phenylene Ethynylene Oligomers and Polymers. Langmuir 27:10770–10775.

17. Hill EH, Pappas HC, Whitten DG. 2014. Activating the antimicrobial activity of an anionic singlet-oxygen sensitizer through surfactant complexation. Langmuir 30:5052–6.

18. Wang Y, Tang Y, Zhou Z, Ji E, Lopez GP, Chi EY, Schanze KS, Whitten DG. 2010. Membrane perturbation activity of cationic phenylene ethynylene oligomers and polymers: selectivity against model bacterial and mammalian membranes. Langmuir 26:12509–12514.

19. Richter SS, Galask RP, Messer SA, Hollis RJ, Diekema DJ, Pfaller MA. 2005. Antifungal susceptibilities of Candida species causing vulvovaginitis and epidemiology of recurrent cases. J Clin Microbiol 43:2155–2162.

20. Pfaller MA, Diekema DJ. 2007. Epidemiology of invasive candidiasis: A persistent public health problem. Clin Microbiol Rev 20:133–163.

21. Ostrosky-zeichner L, Rex JH, Pappas PG, Hamill RJ, Larsen R a, Horowitz HW, Powderly WG, Hyslop N, Kauffman C a, Cleary J, Mangino JE, Lee J. 2003. Antifungal Susceptibility Survey of 2,000 Bloodstream. Society 47:3149–3154.

22. Pfaller MA, Messer SA, Hollis RJ, Jones RN, Diekema DJ. 2002. In Vitro Activities of Ravuconazole and Voriconazole Compared with Those of Four Approved Systemic Antifungal Agents against 6 , 970 Clinical Isolates of Candida spp . Society 46:1723–1727.

23. Cannon RD, Lamping E, Holmes AR, Niimi K, Baret P V., Keniya M V., Tanabe K, Niimi M, Goffeau A, Monk BC. 2009. Efflux-mediated antifungal drug resistance. Clin Microbiol Rev 22:291–321.

24. Sanguinetti M, Posteraro B, Fiori B, Ranno S, Torelli R, Fadda G. 2005.

Mechanisms of Azole Resistance in Clinical Isolates of Candida glabrata Collected during a Hospital Survey of Antifungal Resistance Mechanisms of Azole Resistance in Clinical Isolates of Candida glabrata Collected during a Hospital Survey of Antifungal Re. Society 49:668–679.

25. Perea S, López-ribot JL, Kirkpatrick WR, Mcatee RK, Santillán RA, Marti M, Calabrese D, Sanglard D, Thomas F. 2001. Prevalence of Molecular Mechanisms of Resistance to Azole Antifungal Agents in Candida albicans Strains Displaying High-Level Fluconazole Resistance Isolated from Human Immunodeficiency Virus-Infected Patients Prevalence of Molecular Mechanisms of Resista. Antimicrob Agents Chemother 45:2676–2684.

26. White TC, Marr KA. 1998. Clinical , Cellular , and Molecular Factors That Contribute to Antifungal Drug Resistance. Clin Microbology Rev 11:382–402.

27. Ferrari S, Ischer F, Calabrese D, Posteraro B, Sanguinetti M, Fadda G, Rohde B, Bauser C, Bader O, Sanglard D. 2009. Gain of function mutations in CgPDR1 of Candida glabrata not only mediate antifungal resistance but also enhance virulence. PLoS Pathog 5.

Chapter 2

The Antifungal Properties of Cationic Phenylene Ethynylenes and their Impact on β-Glucan Exposure

2.1 Introduction

Bloodstream infections affect a huge patient population in the United States, with more than 250,000 cases reported each year (1). Patients with indwelling medical devices, such as central venous catheters (CVCs), are most at risk for these infections (2). Frequently, various microorganisms from the skin of the patient, or respective healthcare professional, can gain access through the catheter wound as a result of non-sterile conditions (3–6). Of these resulting bloodstream infections, *Candida* species account for 9% of all instances and are associated with a ~40% mortality rate (2, 7). The most commonly isolated fungal pathogen from bloodstream infections is *Candida albicans*, but the prevalence of other species, such as *C. parapsilosis, C. glabrata*, and *C. tropicalis*, is increasing (8, 9).

An important determinant of pathogenicity among *Candida* spp. is the outer cell wall. The cell wall is primarily composed of carbohydrates and, structurally, is separated into two layers. The outer layer is composed mostly of cell wall glycoproteins with N- and O-linked mannans, and the inner layer is composed of β-glucan and chitin. The complexity of the cell wall contributes to various pathogenic factors including adherence of the fungus and establishment of cross-talk with the host known as “glycan code” (10–12). Cell wall components, such as β-glucan and other polysaccharides, are also found in the extracellular matrix secreted by *Candida* spp. biofilms, which can contaminate the synthetic material surfaces of indwelling medical devices. β-glucan in the extracellular matrix of *Candida* biofilms has been shown to sequester antifungal drugs, which

contributes to decreased drug susceptibility of biofilms (13–15).

Various antimicrobial impregnation approaches have been devised to prevent catheter infections. Catheter materials coated with chlorhexidine-silver sulfadiazine and minocycline/rifampin have shown trends in reduced infection rates, but their clinical effectiveness remains questionable (16, 17). Other treatments, including the use of silver-impregnated subcutaneous collagen cuffs, have also shown to be ineffective in recent trials (18, 19). CVC contamination generally requires device removal and replacement, in addition to a prolonged course of antifungal drug therapy, which raises concerns regarding drug toxicity and the development of antifungal resistance. Antifungal chemotherapy is also problematic, as many antifungal drugs are either toxic to the host (amphotericin B), or result in drug-resistant strains (triazoles) (20). Due to the high morbidity and mortality rate of catheter-related *Candida* spp. bloodstream infections, strategies for preventing medical device contamination by fungal pathogens remain a top priority for infection control.

In this study, we sought to elucidate the antimicrobial effectiveness of two *p*-phenylene ethynylene (PE) compounds against *Candida* species. A subset of conjugated polyelectrolyte, phenylene ethynylenes have shown promising biocidal activity against Gram-positive and -negative bacterial pathogens, as well as the environmental yeast, *Saccharomyces cerevisiae* (21–23). The chemical structure of these compounds renders them capable of inducing broad-spectrum cell damage. The phenylene ethynylenes studied consist of alternating phenyl and acetylenic groups with appended cationic groups (Figure 1). The interaction of the cationic quaternary ammonium groups with net-anionic membranes and cell walls facilitates interactions with microbes, leading to membrane

perturbation, pore formation, and the leakage of cell contents (24). In addition, when PEs are irradiated by the appropriate wavelength, the backbone produces reactive oxygen species (ROS) that induce rapid cell death (25, 26).

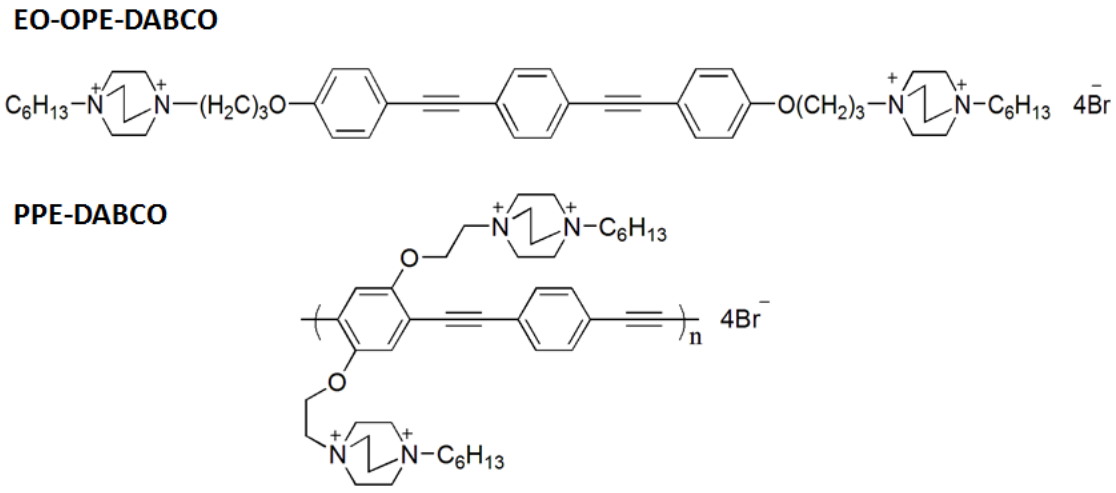

Figure 2: Molecular structures of oligomeric EO-OPE-DABCO (top) and polymeric PPE-DABCO (bottom).

In previous studies, the oligomeric and polymeric molecular size of PE compounds has played an important role in their mechanisms of killing. The antimicrobial activity of these compounds is dependent on various factors that include molecular conformation, size, functional groups, and, of course, membrane composition of the target pathogen (22). The studies described herein serve as a preliminary investigation into the utility of a cationic conjugated polymer, poly(*p*-phenylene ethynylene) and oligomer, “end-only” oligo(*p*-phenylene ethynylene) as antifungals. After treatment with the compounds—hereby referred to as PPE-DABCO and EO-OPE-DABCO—the viability of *Candida* spp. was monitored using flow cytometry. This novel class of compounds may provide an

innovative approach to preventing catheter-related bloodstream infections caused by *C. albicans* and other *Candida* species.

2.2 Materials & Methods

Fungal Culture

Candida albicans (ATCC, #MYA-2876), *C. parapsilosis* (ATCC, #22019), and *C. glabrata* (ATCC, #2001) were grown from glycerol stocks, stored at -80 °C. Said stock was transferred to 5 mL filter-sterilized yeast extract-peptone-dextrose (YPD) medium (Becton Dickinson), and grown for 16 h at 30 °C, with a shaking speed of 300 RPM. Such growth conditions yielded yeast at the late log phase (27).

Following a 10 minute centrifugation at 2,900 rcf, the supernatant was replaced with sterile phosphate-buffered saline (PBS), and subsequently vortexed. This washing step is repeated a second time to mitigate cell debris. Cell concentration was then determined using a disposable hemocytometer (INCYTO C-Chip; Fisher Scientific).

Derivation of Clinical Isolate Strains of C. albicans

Patient specimens (peripheral blood or catheter tips) were processed by Tricore Reference Laboratories (Albuquerque, NM) and identified as *C. albicans* using a Bruker Biotyper MALDI-TOF system (MS ID score > 2.0). Clonal isolates so identified were subcultured on Sabouraud agar slants and provided to the investigators as unique strains. Isolate strains were provided in completely deidentified form according to procedures approved by the University of New Mexico School of Medicine Human Research

Protections Office. For biocidal assays, clinical isolates were grown in YPD broth as described above.

Biocidal Testing

All biocidal experiments were carried out in either translucent or opaque 1.5 mL microcentrifuge tubes, at cell concentrations of 5 x 10^6/mL. Two cationic compounds were tested, both based on the *p*-phenylene ethynylene backbone, with quaternized diazabicyclo[2,2,2]octane (DABCO)-functionalities. EO-OPE-DABCO and PPE-DABCO stocks were prepared in sterile deionized water (18.2 MΩ·cm at 25 °C), and contained 0.47% dimethyl sulfoxide (by volume) to improve solubility and minimize aggregate formation. Negative controls contained equal amounts of dimethyl sulfoxide.

Samples were exposed to controlled amounts of light using a 14-lamp photoreactor (LZC-4V; Luzchem Research; Ottawa, Ontario). A rotating carousel ensured that all samples receive equivalent levels of light exposure; ventilation kept the photoreactor below 30 °C. EO-OPE-DABCO absorbs in the ultraviolet region (28), warranting the use of UVA lamps (350 nm emission peak; 4.46 ± 2.41 mW/cm^2) to optimize singlet oxygen yields. Conversely, 420 nm blue-light lamps (6.62 ± 2.93 mW/cm^2) were used in PPE-DABCO tests; unlike its oligomeric counterpart, polymeric PPE-DABCO absorbs in the near-visible range (29). Power density output was measured at the peak excitation wavelength for both lighting configurations. Data shown is an aggregation of two independent replicate experiments.

Samples were then stained with 5 μM membrane-permeable SYTO 9 (Invitrogen, S34854) and 1 μM membrane-impermeable TO-PRO-3 (Invitrogen, T3605), both of which

are nucleic acid stains. After 30 min, samples were evaluated by flow cytometry (FACSCalibur; Becton Dickinson). At least 10,000 events were evaluated in each trial. A heat-killed sample (70 °C for 30 min) was used to identify the fluorescence characteristics of dead cells.

15 min dark-activity assays were carried out in a somewhat different manner. Samples were prepared and stained with SYTO 9 and TO-PRO-3, albeit in the absence of any biocide. After a 30 min staining duration, EO-OPE-DABCO was added (10 µg/mL final concentration); the sample was then vortexed and analyzed by flow cytometry. Every minute, viability data was collected (again, 10,000 events/sample), for a total of 15 minutes. It is important to note that EO-OPE-DABCO was added one sample at a time, so that, in each case, flow cytometry readings could begin within 1 min of the biocide's introduction.

Spectroscopy of β-glucan Interactions

Stocks of *S. cerevisiae* β-(1,3)-glucan (high, medium or low MW; gift of Biothera, Eagan, MN), PPE-DABCO, and EO-OPE-DABCO were mixed with 10 mM pH 7.4 phosphate buffer to a final concentration of 2 µg/mL in PPE-DABCO or EO-OPE-DABCO and 100 µg/mL in β-glucan. 200 µL solutions were transferred to a 160 µL nominal volume fused quartz fluorimetry cuvette, and read on a PTI QuantaMax 40 steady-state fluorescence spectrophotometer (HORIBA Scientific, Edison, NJ) with PMT detection. Emission spectra were obtained using an excitation wavelength of 350 nm for EO-OPE-DABCO and 420 nm for PPE-DABCO, and excitation spectra were obtained with the corresponding maximum emission wavelength.

Interactions of PPE-DABCO with Glucan Microparticles

Glucan microparticles were prepared from *Candida* yeast cells using the extraction techniques disclosed Lowman *et al* (30). Glucan microparticles were then suspended in PBS at a concentration of 1 x 10^5 mL^{-1}. Microparticles were sonicated for 10 min, and subsequently vortexed for another 5 min. PPE-DABCO was then added at a concentration of 2 µg/mL, and incubated at room temperature for 1 h. No PPE-DABCO was added to the negative control. 500 µL of each sample was transferred to petri dishes for examination by confocal microscopy. 405 nm excitation was used to induce fluorescence of PPE-DABCO.

Surface Exposure of β-glucan

C. albicans yeast cells were treated in a similar manner to that of the previously described biocidal experiments. In effort to maintain a consistent degree of cell death across samples, OPE-DABCO exposure in UVA light was limited to just 10 min. A thermal positive control was also implemented, which entailed heating samples to 100 °C for 30 min. Following the appropriate treatment and removal from the photoreactor, samples were blocked with 1% (w/v) bovine serum albumin (BSA) for 30 min at room temperature. The samples were then treated with a primary antibody, anti β-glucan IgG (Biosupplies, 400-2), at a final concentration of 10 µg/mL, for an additional 30 min. Negative controls contained 10 µg/mL isotype-matched murine IgG in place of anti β-glucan IgG. A secondary antibody with Alexa Fluor 647 dye (Invitrogen, A21235) was then added (1 µg/ml in PBS+1% BSA), along with 5 µM SYTO 9 were simultaneously added and allowed

to stain cells for 30 minutes at 25 °C prior to analysis by flow cytometry. Data shown is an aggregation of two independent replicate experiments.

Tissue Culture & Transfection

HEK-293 cells (ATCC, #CRL-1573) were cultured in DMEM supplemented with 10% CS, 1% Penicillin/Streptomycin, 2mM L-glutamine, and 1mM sodium pyruvate at 37°C, 5% CO_2. Cells were then plated in 6 well plate at $1x10^5$ cell per well. mApple-human Dectin1A-C-10 (gift of Michael Davidson, Addgene #54883) was transfected into cells by following standard protocols using Fugene 6 (Promega, #E2691). Cell cultures were used for further experimentation at 24 h post-transfection with growth in normal medium, as described above.

Phagocytosis Assay

C. albicans yeast cells were subjected to the same treatment conditions as in the aforementioned β-glucan exposure study, before being spun down and washed in PBS. Following the last wash step the *C. albicans* were stained with 7.5μM of SYTO 9 (Invitrogen, #S-34854) and 75μM of CypHer5E NHS-ester (GE Healthcare, #PA15401) for one hour at 25°C. After staining the *C. albicans* were added to live, Dectin-1A-C-10 transfected HEK-293 cells for one hour. Next ice cold PBS was used to lift the HEK-293 cells off of the plate. The controls with *C. albicans* or HEK-293 alone or the above samples with a mixture of *C. albicans* and HEK-293 cells were analyzed using an LSR Fortessa flow cytometer (Becton Dickinson) and FlowJo software (FlowJo, Ashland, OR). At least 10,000 side scatter (SSC)-positive events are evaluated in each trial. CypHer 5, SYTO 9, and mApple fluorescence was observed at emission wavelengths of 660 nm

(670/14), 525 nm (505 LP, 530/30), and 578 nm (582/15), respectively. Data shown is an aggregation of two independent replicate experiments.

2.3 Results

A series of biocidal studies were carried out to gain insight to the light-activated effects of EO-OPE-DABCO and PPE-DABCO on *Candida* species pathogens. Phenylene ethynylenes are unique in that their mechanism of action differs, depending on the presence of light; in particular, light intensity, emission wavelength, and duration (31). In the studies described herein, duration of light exposure was the primary variable being studied. Light intensity was kept constant using a photoreactor with 14 interchangeable lamps. Lamps were chosen to have an emission wavelength overlapping the excitation spectrum of the phenylene ethynylene being used. 350 nm-centered UVA lamps were implemented for OPE testing, while 420 nm-centered lamps were used in PPE tests. With light intensity and spectrum being held constant for a given phenylene ethynylene, we focused on light exposure duration as the major focal point in an effort to discern *C. albicans'* susceptibility to phenylene ethynylenes in the light vs. dark. Even though all samples were exposed to one of the two compounds for a total of 60 min, the duration of light exposure was varied by 4 min intervals and the balance of 60 min exposure was in the dark.

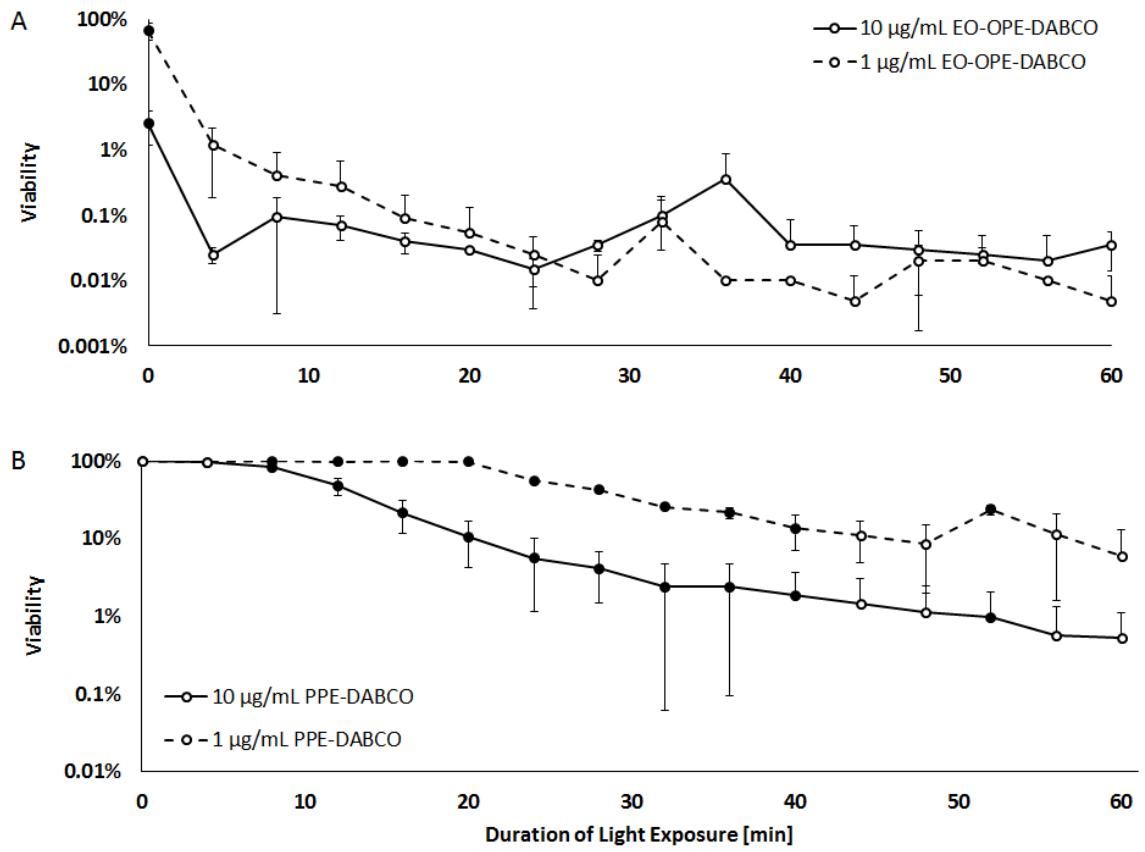

Figure 3: *C. albicans* yeast viability as a function of light exposure duration and antimicrobial concentration. Viability is shown on a logarithmic scale for EO-OPE-DABCO (A) or PPE-DABCO (B) at 1 µg/ml (dashed lines) or 10 µg/ml (solid lines). Significant differences in viability are indicated by filled data markers (P-value ≤ 0.01).

Fig. 2A illustrates the biocidal activity of the two concentrations of EO-OPE-DABCO: 1 and 10 µg/mL. In the absence of light, a 1 µg/mL concentration of OPE killed 34% of *C. albicans* yeast cells; however, killing drastically increased with just minimal light exposure, as 2 log cell death was observed after just 8 min. Increasing the concentration to 10 µg/mL greatly improved the dark killing capacity of the OPE, resulting in 97% cell death. With minimal light exposure, 10 µg/mL EO-OPE-DABCO exhibited a profound biocidal

effect, exceeding 3 log reduction after just 4 min in UVA light. Both OPE concentrations exceeded 3 log kill (over 99.9% cell death) after 20 min of light exposure, and 4 log reduction (99.99% cell death) is nearly achieved after 60 min of light exposure. Interestingly enough, lowering the concentration of OPE to just 1 μg/mL had little effect on light-activated biocidal activity, but a far larger effect on dark killing. Some level of PE photodegradation was notable by 60 min (data not shown), which is why testing durations were limited to 1 h, as photodegradation limits $^1O_2$ generation.

Fig. 2B illustrates the viability of *C. albicans* following exposure to PPE-DABCO. It is quite evident that, unlike EO-OPE-DABCO, its PPE counterpart is non-toxic in the absence of light; even at a relatively high concentration of 10 μg/mL, little-to-no cell death was observed even after 8 min of exposure to 420 nm light. After 52 min of continuous light exposure, 10 μg/mL PPE was able to kill 99% of all *C. albicans* yeast cells. In summary, we find the dark killing of the OPE to be concentration-dependent, while the light activity is not. Conversely, the PPE's dark killing was not dependent on concentration, since it failed to elicit membrane damage in that case. Biocidal activity of PPE-DABCO is predicated on light exposure.

PPE-DABCO's inability to kill *C. albicans* in the dark led us to question whether the polymer may bind extensively to cell wall components, which could limit its ability to access the cell membrane. We evaluated the interactions between both PEs with soluble β-(1,3)-glucan extracted from *Saccharomyces cerevisiae* yeast cell walls (32). The structure of *S. cerevisiae* and *C. albicans* β-(1,3)-glucan is quite similar, and this polysaccharide is an important part of *Candida* drug resistance and pathogenicity, amounting to 40% of the cell wall (33). Size fractionated β-glucan (low MW = 11 kDa,

medium MW = 150 kDa, high MW = 450 kDa) were tested (Fig. 3 A-D, Fig. S1). Excitation and emission spectra of EO-OPE-DABCO and PPE-DABCO were evaluated in the absence or presence of the soluble β-glucan.

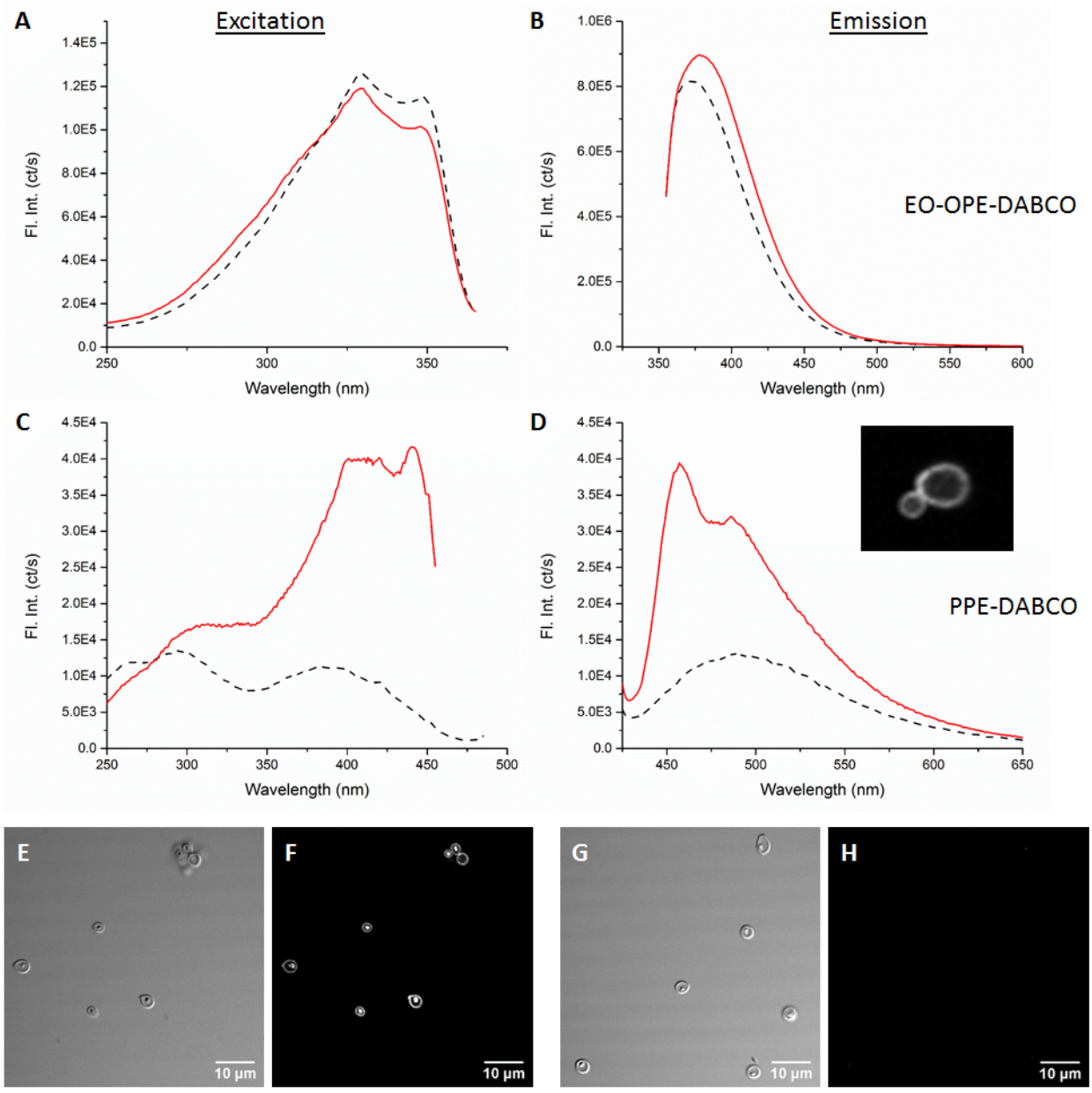

Figure 4: Excitation (A, C) and emission (B, D) spectra illustrating the interactions between high molecular weight soluble β-glucan and EO-OPE-DABCO (top) or PPE-DABCO (bottom). Dashed lines represent spectra of PE compounds alone, and solid lines represent the spectra observed in PE/β-glucan mixtures. Inset illustrates fluorescent

PPE-DABCO concentrated in the cell wall of a *C. albicans* yeast cell, as shown in Fig. S2. Additionally, confocal microscopy images illustrate PPE-DABCO bound to glucan microparticles. A transmitted light image (E) and reflected light image (F) are shown, with 405 nm excitation being used to generated fluorescence of bound PPE-DABCO. No fluorescent signal is observed in the absence of PPE-DABCO (G, H).

We observed enhanced emission of both PEs upon the introduction of the high molecular weight β-glucan, which is indicative of complexation (34). Emission enhancement is more profound in the case of PPE-DABCO (Fig. 3 A-D), suggesting that complexation with soluble β-glucan promotes disaggregation of the PE polymer. In addition, a small degree of red-shifting was observed, implying that rotation of the conjugated regions of the PEs is restricted due to complexation with soluble β-glucan (35). The complexation between PPE-DABCO and β-glucan suggests that it may be largely sequestered in the cell wall; such positioning promotes interaction with components of the outer cell wall, but may limit its ability to directly disrupt the plasma membrane.

These results shed light onto the mechanisms by which EO-OPE-DABCO kills *C. albicans* yeast cells (Fig. 2A; see discussion). With this in mind, the OPE became a focal point of this study, from a biocidal perspective. Having determined that EO-OPE-DABCO was highly effective at killing standard lab-strain *C. albicans* (SC5314), the question remained whether or not its biocidal efficacy would carry over to *C. albicans* clinical isolates.

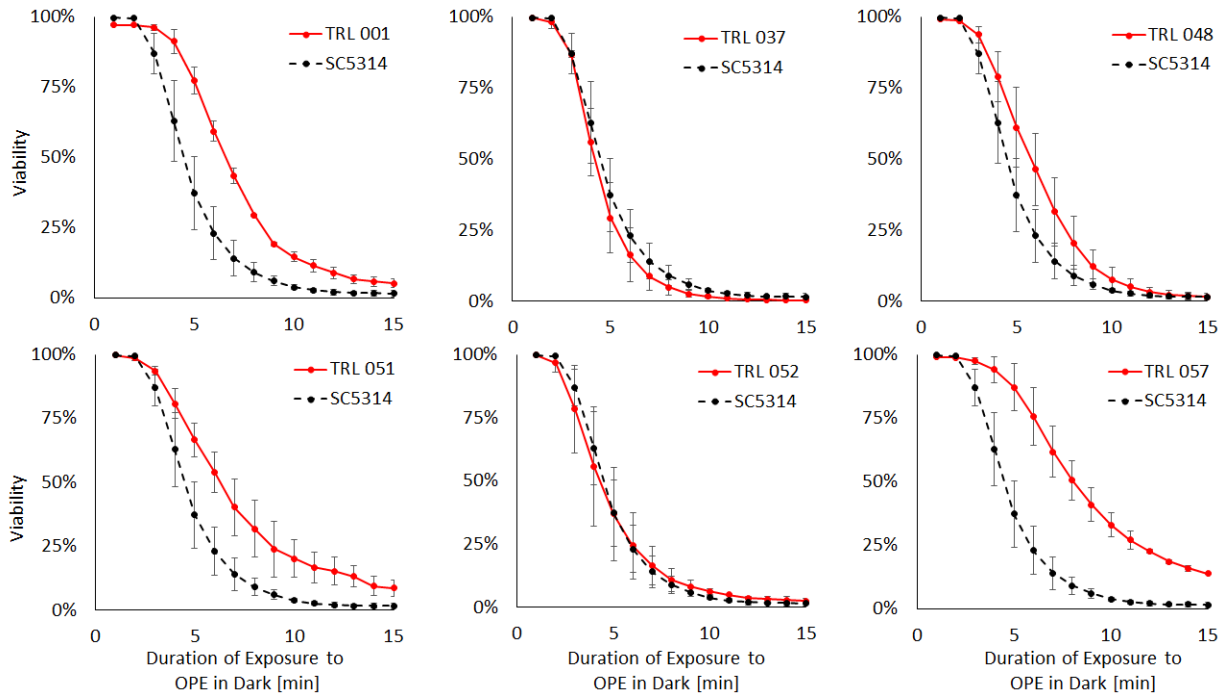

Figure 5: Susceptibility of various *C. albicans* clinical isolates to 10 µg/mL EO-OPE-DABCO in the dark. Lab strain SC5314 is shown for reference in all cases. Strains prefixed "TRL" are recent (circa 2015) clinical isolates obtained as described in *Materials and Methods*.

Using a modified biocidal assay, six *C. albicans* clinical isolates were surveyed for their susceptibility to 10 µg/mL EO-OPE-DABCO in the dark. In this instance, the cells were stained with SYTO 9 and TO-PRO-3 before the introduction of EO-OPE-DABCO. Taking a flow cytometry dual-fluorescent measurement of 10,000 events every minute allowed for real-time reporting of OPE-induced membrane perturbation. The susceptibility of clinical isolates was gauged relative to that of *C. albicans* SC5314, as shown in Fig. 4. Three of the six isolates, TRL 001 (P-Value = 0.006), 051 (P-Value = 0.0013), and 057 (P-Value = 0.0003) showed significantly increased levels of OPE-resistance within 15

minutes' time in the form of slower kinetics of killing and higher residual viability after 15 minutes of treatment. Conversely, no OPE-resistance was observed in TRL 037, 040, and 052.

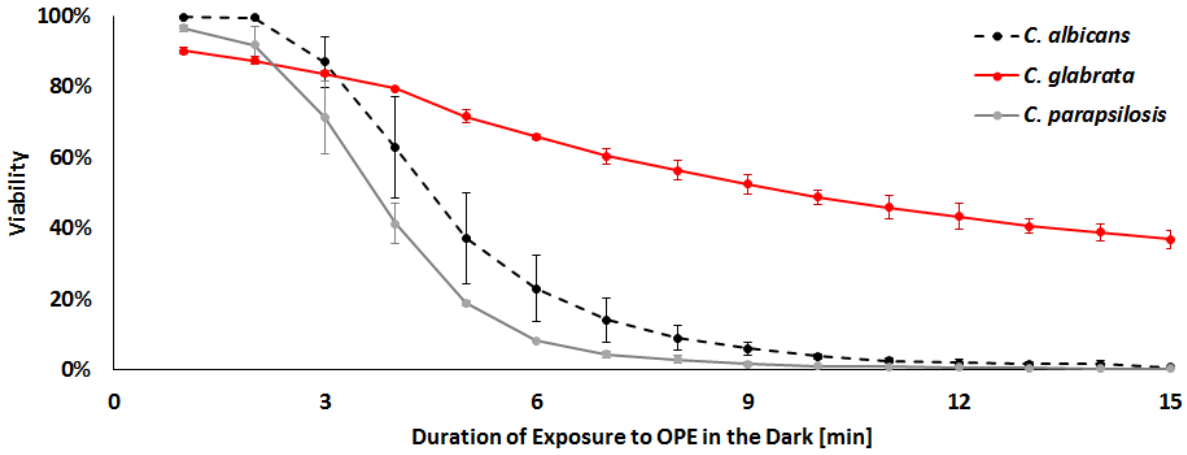

Figure 6: Viability of *C. albicans*, *C. glabrata*, and *C. parapsilosis* in the presence of 10 µg/mL EO-OPE-DABCO in the dark.

Variability of susceptibility to EO-OPE-DABCO amongst clinical isolates of one species (*C. albicans*) suggested that non-*albicans Candida* species pathogens might also exhibit variable sensitivity to this biocide. To test this, we revised the aforementioned 15 min flow cytometry assay to determine if EO-OPE-DABCO was more or less effective against *C. parapsilosis* and *C. glabrata* relative to *C. albicans* SC5314. Fig. 5 shows similar degrees of biocidal activity against *C. albicans* and *C. parapsilosis*, but less activity against *C. glabrata*, with about 50% surviving through 15 min' exposure. This result is consistent with the fact that *C. albicans* and *C. parapsilosis* share a closer phylogenetic relationship than is found between *C. albicans* and *C. glabrata* (36).

β-glucan is highly immunogenic upon recognition by the innate immunoreceptors Dectin-1 or Mac-1 (37). Several prominent genera of fungal pathogens, including *Candida*, are known to employ an innate immune evasive strategy of masking β-glucan to restrict its exposure on the cell wall surface (38–41). We hypothesize that PE antimicrobials bound to cell wall constituents and exposed to light will generate singlet oxygen, leading to local cell wall damage, unmasking β-glucan and increasing immunogenicity. Using an anti-β-(1,3)-glucan primary antibody in tandem with a secondary fluorescently-labeled antibody allowed for the comparison of β-glucan exposure following treatment conditions: PE in the dark, PE in the light, and a 60 min light negative control. *C. albicans* yeast treated with EO-OPE-DABCO in the dark, using conditions associated with high biocidal activity (Fig. 2), exhibited no increase in β-glucan exposure. Likewise, we observed no β-glucan unmasking with light-activated EO-OPE-DABCO. We then treated *C. albicans* with PPE-DABCO and observed β-glucan exposure. PPE-DABCO clearly binds to the fungal cell wall as evidenced by strong PPE-DABCO emission upon 405 nm excitation using confocal imaging (Fig. S2). In the absence of stimulation by light, PPE-DABCO treatment results in no significant increase in β-glucan exposure. After illumination, PPE-DABCO treated cell walls do show evidence of significant β-glucan unmasking (Fig. 6). These results suggested that β-glucan masking in *Candida* cell walls is light-dependent and, presumably, mediated by $^1O_2$ and other ROS.

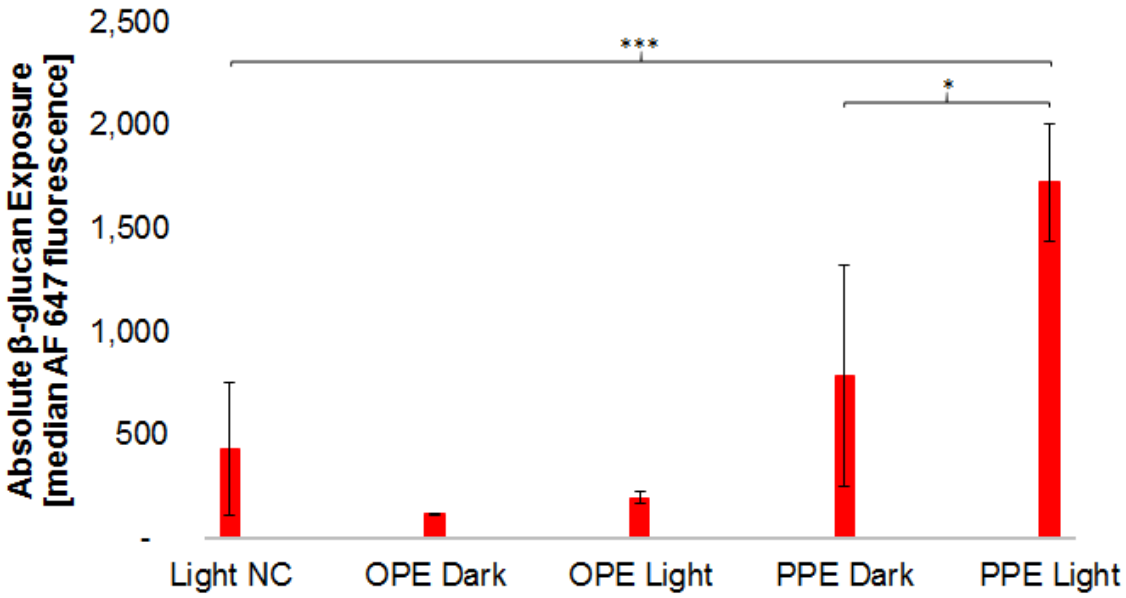

Figure 7*:* Absolute β-glucan exposure of *C. albicans* following various treatments. β-glucan exposure estimated from median fluorescence signal of AF 647. The exposure duration of all samples was 60 min, with the exception of EO-OPE-DABCO exposure in the light, for which the exposure duration was limited to 10 min.

Given the evidence that PPE-DABCO can increase β-glucan exposure on *C. albicans* yeast, we tested whether the unmasking achieved by this treatment resulted in greater recognition of yeasts through the β-glucan receptor Dectin-1. HEK-293 cells were transfected with mApple-tagged human Dectin-1a, whereby expression is sufficient to drive phagocytosis of *C. albicans* yeast cells (42). Our transfection conditions resulted in Dectin-1^{+} HEK-293, discriminated by positive mApple signal, and non-transfected cells, which were negative for mApple and served as an internal control to assess Dectin-1 dependence of binding and phagocytosis. We employed a flow cytometric assay of yeast cell binding to and internalization by HEK-293 transfectants. Yeasts were labeled with

the pH-sensitive dye CypHer 5, which increases dramatically in emission intensity after internalization within acidic phagosomal compartments (43, 44). The Cypher 5 signal was used to measure binding and internalization of yeast. Flow cytometry data were gated on HEK-293 cell-containing events for analysis, as defined by high side scatter signal, which was significantly larger than free yeast. Yeast bound to HEK-293 cells registered a low Cypher 5 signal. If yeasts were internalized, the CypHer 5 signal was much higher. The percent of HEK-293 cells with yeast bound (for mApple-Dectin-1^{+} and mApple-Dectin-1^{-} cells) was determined by the percent of SSC-gated events having low or high CypHer 5 signal. The extent of phagocytosis was assessed by the median CypHer 5 fluorescence intensity within these populations (Fig. S3).

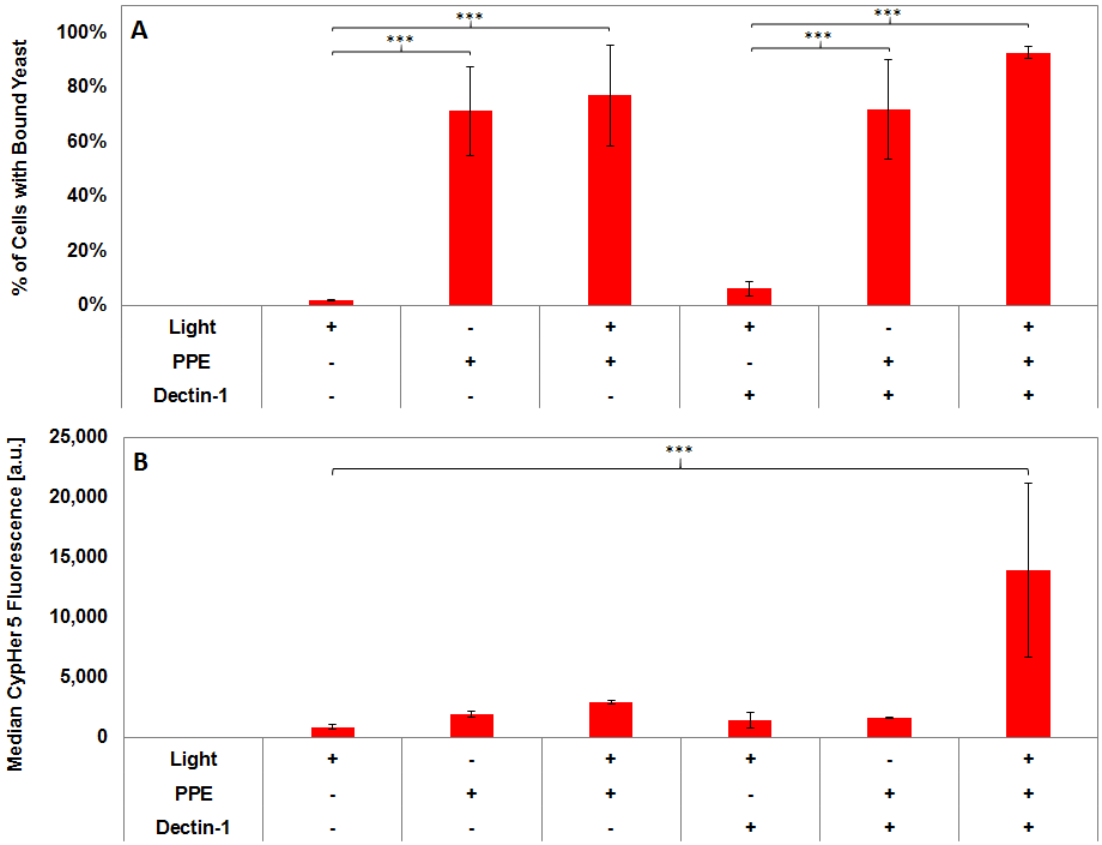

Figure 8: PPE-DABCO induces *C. albicans* yeast phagocytosis by HEK-293 cells in a manner that requires illumination of PPE-DABCO and expression of the β-glucan receptor Dectin-1. Prior to the addition of HEK cells, samples were first treated with 10 μg/mL PPE-DABCO for 1 h and subsequently stained with CypHer 5 and SYTO 9. A) PPE-DABCO treatment, with or without illumination, induces increased binding of *C. albicans* to HEK-293 cells in a Dectin-1 independent fashion. B) Phagocytosis of *C. albicans* yeast bound to HEK-293 cells requires Dectin-1 expression and is induced by light treatment of PPE-DABCO.

As can be seen in Fig. 7, we observe minimal binding between mApple-Dectin-1$^-$ HEK-293 cells and untreated *C. albicans* yeast cells. Even if the HEK-293 cell has been transfected and is expressing Dectin-1 (mApple+), β-glucan masking permits very little β-glucan to be accessible at the cell wall surface for Dectin-1 binding (as seen in Fig. 6). Conversely, PPE-treated *C. albicans* yeast cells bind avidly to HEK-293 cells, and this binding is independent of excitation of PPE-DABCO or Dectin-1 expression by the HEK-293 (Fig. 7A). These data suggest that the binding of PPE-DABCO to *Candida* cell walls alters their surface properties in ways that promote Dectin-1 independent adhesion to human cells, perhaps through electrostatic and/or hydrophobic mechanisms. The extent of interaction between the yeast cell and the HEK-293 cell is not dependent on the degree of incurred cell membrane damage, as *C. albicans* killed with light-activated PPE were no more likely to bind HEK-293 cells. Despite their ability to bind HEK-293, internalization of PPE-DABCO-treated *C. albicans* yeasts required Dectin-1 expression and excitation of PPE-DABCO prior to binding (Fig. 7B). These data indicate that the β-glucan unmasking caused by light-activation of PPE-DABCO on *C. albicans* cell walls results in the biological outcome of increased Dectin-1 dependent phagocytosis.

2.4 Discussion

Cationic Phenylene Ethynylenes Exhibit Biocidal Effects against Candida *Yeast*

Despite their intrinsic resistance to cationic and oxidative stresses, (45, 46) *C. albicans* was highly susceptible to EO-OPE-DABCO, and to a lesser extent, PPE-DABCO. Biocidal activity of these compounds against *C. albicans* utilizes a dual mechanism combining light-independent cationic stress and light-dependent oxidative stress. These

results resemble those of previous studies, which demonstrate the effectiveness of a dual-mechanism mode of biocidal action (47). Unlike other broad-spectrum antimicrobials, PEs exhibit low levels of *in vitro* toxicity against mammalian cells (48), making them attractive candidates in numerous clinical applications.

Therefore, it is relevant to note that all clinical isolate strains exhibited significant amounts of killing during a 15 min exposure to EO-OPE-DABCO. Partial resistance of some clinical isolate strains may derive from adaptations of the pathogen to growth in the host, which may cause changes in cell wall structure and upregulation of mechanisms that permit growth under adverse conditions, such as leukocyte-derived ROS in the phagosomal environment (49, 50). Previous research has also suggested a correlation between *Candida* resistance to the antifungal drug amphotericin B and cell wall structure and composition (51, 52).

While *C. parapsilosis* was found to be as susceptible to EO-OPE-DABCO in the dark as *C. albicans*, *C. glabrata* displayed an inherent resistance. *Candida* spp. experience cationic stress as they interact with innate immune defenses. For example, cationic antimicrobial peptides, such as Histatnin-5, are deployed in host defense against *Candida* spp. and are thought to work by disrupting fungal plasma membrane integrity (53). *C. glabrata* is noted for its resistance to killing by cationic antimicrobial peptides relative to *C. albicans* and other *Candida* spp. pathogens (54–56). Furthermore, EO-OPE-DABCO's decreased ability to kill *C. glabrata* resembles the results of a previous study, in which a 10 μg/mL concentration of the compound failed to kill 99% of *S. cerevisiae* yeast, even after an hour in the light (23). Although *S. cerevisiae* is benign, it is closely related to *C. glabrata* (32, 36). Finally, *C. glabrata* is also known to have robust

antioxidative defenses that allow it to survive in the phagosome (57, 58), and may impact its ability to resist oxidative killing by cationic phenylene ethynylenes.

Interactions with β-glucan

An interesting result of this study is that PPE-DABCO strongly associates with soluble β-(1,3)-glucan (Fig. 3 C-D), which is important for structural support of the cell wall of *C. albicans* (32), as well as glucan microparticles (Fig. 3 E-F). We speculate that PPE-DABCO/β-glucan interaction may directly cause more global disruption to the cell wall, and it is likely that the targeting of polymeric phenylene ethynylenes to cell wall polysaccharides places them in an ideal position to exhibit reactive oxygen-mediated damage to cell wall components after photoactivation. Using transmission electron microscopy and other techniques, Wang *et al.* demonstrated this behavior with PPE-DABCO and Gram-negative *Escherichia coli* (31). However, we also note the alternative possibility that glucan exposure upon PPE-DABCO/light treatment might require cell wall remodeling downstream of cell wall stress responses due to ROS generated by excited PPE-DABCO.

Conversely, the OPE appears far less prone to complexation with the soluble β-(1,3)-glucan. Although this may limit the OPE's ability to unmask mannoproteins and reveal more β-(1,3)-glucan (Fig. 6), the lack of interaction with the glucan likely allows the molecule to quickly penetrate the cell wall, access and damage the cell membrane. Abundant lateral non-covalent interactions between β-glucan and PPE-DABCO may promote PE/β-glucan complexation, analogous to the role of interpolymeric hydrogen bonding in stabilizing lateral interactions of individual β-glucan polymers in aqueous

solution (59, 60). PPE-DABCO is far larger than its oligomeric counterpart, and has numerous sites where weak interactions with β-glucan polymers may form; furthermore, extensive valency of laterally-aggregated β-glucan would make this interaction very strong. Emission enhancement of the PE polymer (Fig. 3) resembles that of a previous study, by which PPE-DABCO was shown to exhibit similar photophysical effects in methanol, as opposed to water (29). Therefore, we suggest that abundant complexation with soluble β-glucan disaggregates PPE-DABCO in aqueous buffer.

These results help in justifying the PPE's inability to kill *C. albicans* in the dark. Exhibiting a strong propensity to interact and associate with β-glucan, it is likely that PPE-DABCO is limited in its ability to fully penetrate the cell wall and much of the compound is sequestered on β-glucan in the cell wall. Given the limited radius of destruction of singlet oxygen and the density of organic material in the cell wall capable of quenching singlet oxygen, this association may be limiting the depth of cell wall permeation of PPE-DABCO and its capacity to directly perturb the yeast's plasma membrane, relative to EO-OPE-DABCO. However, an advantage of PPE-DABCO's ability to bind β-glucan may be an increased specificity and targeting to the fungal pathogen's cell wall as opposed to host tissues, which are devoid of β-glucan. The oligomer, on the other hand, appears far less likely to interact with β-glucan, which may allow it to permeate the fungal cell wall more readily and better access the yeast's plasma membrane.

PPE-DABCO Unmasks β-glucan

Furthermore, PPE-DABCO displays immunostimulatory attributes, particularly in the light. This polymer was found to unmask the outer cell wall of *C. albicans* yeast cells in such a

way that β-(1,3)-glucan could more easily be recognized and bound by pattern recognition receptor Dectin-1. PPE-DABCO binds to yeast cell walls (Fig. S2). The chemical basis of this binding may relate to direct interactions between PPE-DABCO and β-(1,3)-glucan, as discussed above. Additionally, PPE-DABCO may interact electrostatically with anionic moieties in the outer cell wall. Ultrastructural studies have described the presence of evenly-dispersed anionic sites on the *C. albicans* yeast surface (61). Also, *C. albicans* N-linked mannans contain abundant oligomannose side chains attached via anionic phosphodiester linkages that could provide sites of electrostatic binding for polycations like PPE-DABCO (62, 63). In either configuration, PPE-DABCO would be ideally positioned in the outer cell wall to damage mannoproteins that are thought to provide β-glucan masking. Our results suggest that merely the binding of PPE-DABCO to *C. albicans* increases adherence of yeast to HEK-293 cells in a receptor-independent fashion, suggesting that PPE-DABCO alters cell wall surface characteristics in ways that impact interaction with host cells non-specifically (Fig. 7A). However, increases in both β-glucan exposure and Dectin-1-dependent phagocytosis require excitation of PPE-DABCO, which probably results in direct oxidative damage to the cell wall leading to β-glucan unmasking. This is the first instance in which PEs have been demonstrated to elicit immunostimulatory attributes. Our work demonstrates that the biocidal and immunostimulatory properties of phenylene ethynylene antimicrobials make them promising candidates for novel antimicrobial applications to improve the health outcomes of patients with life-threatening fungal infectious diseases.

.

References

1. Maki DG, Kluger DM, Crnich CJ. 2006. The Risk of Bloodstream Infection in Adults With Different Intravascular Devices: A Systematic Review of 200 Published Prospective Studies. Mayo Clin Proc 81:1159–1171.
2. Wisplinghoff H, Bischoff T, Tallent SM, Seifert H, Wenzel RP, Edmond MB. 2004. Nosocomial bloodstream infections in US hospitals: analysis of 24,179 cases from a prospective nationwide surveillance study. Clin Infect Dis 39:309–317.
3. Snydman DR, Gorbea HF, Pober BR, Majka JA, Murray SA PL. 1982. Predictive value of surveillance skin cultures in total-parenteral-nutrition-related infection. Lancet 320:1385–1388.
4. Bjornson, H. S., Colley, R., Bower, R. H., Duty, V. P., Schwartz-Fulton, J. T., & Fischer JE. 1982. Association between microorganism growth at the catheter insertion site and colonization of the catheter in patients receiving total parenteral nutrition. Surgery 92:720–727.
5. Cooper, G.L. and Hopkins C. 1985. Rapid diagnosis of intravascular catheter-associated infection by direct Gram staining of catheter segments. N Engl J Med 312:1142–1147.
6. Raad, I., Costerton, W., Sabharwal, U., Sadlowski, M., Anaissie, E. and Bodey GP. 1993. Ultrastructural analysis of indwelling vascular catheters: a quantitative relationship between luminal colonization and duration of placement. J Infect Dis 168:400–407.
7. Edmond MB, Wallace SE, McClish DK, Pfaller MA, Jones RN, Wenzel RP. 1999. Nosocomial bloodstream infections in United States hospitals: A three-year analysis. Clin Infect Dis 29:239–244.
8. Wingard JR. 1995. Importance of Candida species other than C. albicans as pathogens in oncology patients. Clin Infect Dis 20:115–125.
9. Giri, S., & Kindo AJ. 2012. Review of Candida species causing blood stream infection. Indian J Med Microbiol 30:270.
10. Ruiz-Herrera J, Elorza MV, Valentín E, Sentandreu R. 2006. Molecular organization of the cell wall of Candida albicans and its relation to pathogenicity. FEMS Yeast Res 6:14–29.
11. Klis FM, Groot PDE, Hellingwerf K. 2001. Molecular organization of the cell wall of Candida albicans 1–8.
12. Netea MG, Gow NAR, Munro C a., Bates S, Collins C, Ferwerda G, Hobson RP, Bertram G, Hughes HB, Jansen T, Jacobs L, Buurman ET, Gijzen K, Williams DL,

Torensma R, McKinnon A, MacCallum DM, Odds FC, Van Der Meer JWM, Brown AJP, Kullberg BJ. 2006. Immune sensing of Candida albicans requires cooperative recognition of mannans and glucans by lectin and Toll-like receptors. J Clin Invest 116:1642–50.

13. Kojic EM, Darouiche RO. 2004. *Candida* Infections of Medical Devices. Clin Microbiol Revi 17:255–267.

14. Nett JE, Andes DR. 2015. Fungal Biofilms: In Vivo Models for Discovery of Anti-Biofilm Drugs. Microbiol Spectr 3.

15. Mitchell KF, Taff HT, Cuevas MA, Reinicke EL, Sanchez H, Andes DR. 2013. Role of matrix β-1,3 glucan in antifungal resistance of non-albicans Candida biofilms. Antimicrob Agents Chemother 57:1918–20.

16. Brun-Buisson C, Doyon F, Sollet J-P, Cochard J-F, Cohen Y, Nitenberg G. 2004. Prevention of intravascular catheter-related infection with newer chlorhexidine-silver sulfadiazine-coated catheters: a randomized controlled trial. Intensive Care Med 30:837–43.

17. Ramritu P, Halton K, Collignon P, Cook D, Fraenkel D, Battistutta D, Whitby M, Graves N. 2008. A systematic review comparing the relative effectiveness of antimicrobial-coated catheters in intensive care units. Am J Infect Control 36:104–117.

18. Kalfon, P., De Vaumas, C., Samba, D., Boulet, E., Lefrant, J.Y., Eyraud, D., Lherm, T., Santoli, F., Naija, W. and Riou B. 2007. Comparison of silver-impregnated with standard multi-lumen central venous catheters in critically ill patients*. Crit Care Med 35:1032–1039.

19. Groeger JS. Lucas AB. Coit D. LaQuaglia M. Brown AE. Turnbull A. Exelby P. 1993. A prospective, randomized evaluation of the effect of silver impregnated subcutaneous cuffs for preventing tunneled chronic venous. Ann Surg 218:206–210.

20. Perfect JR. 2004. Antifungal resistance: the clinical front. Oncology (Williston Park) 18:15–22.

21. Zhou Z, Corbitt TS, Parthasarathy A, Tang Y, Ista LK, Schanze KS, Whitten DG. 2010. “End-Only” Functionalized Oligo(phenylene ethynylene)s: Synthesis, Photophysical and Biocidal Activity. J Phys Chem Lett 1:3207–3212.

22. Wang Y, Zhou Z, Zhu J, Tang Y, Canady TD, Chi EY, Schanze KS, Whitten DG. 2011. Dark Antimicrobial Mechanisms of Cationic Phenylene Ethynylene Polymers and Oligomers against Escherichia coli. Polymers (Basel) 3:1199–1214.

23. Wang Y, Chi EY, Natvig DO, Schanze KS, Whitten DG. 2013. Antimicrobial activity

of cationic conjugated polyelectrolytes and oligomers against Saccharomyces cerevisiae vegetative cells and ascospores. ACS Appl Mater Interfaces 5:4555–61.

24. Wang Y, Jones EM, Tang Y, Ji E, Lopez GP, Chi EY, Schanze KS, Whitten DG. 2011. Effect of Polymer Chain Length on Membrane Perturbation Activity of Cationic Phenylene Ethynylene Oligomers and Polymers. Langmuir 27:10770–10775.

25. Hill EH, Pappas HC, Whitten DG. 2014. Activating the Antimicrobial Activity of an Anionic Singlet-Oxygen Sensitizer through Surfactant Complexation. Langmuir 30:5052–6.

26. Wang Y, Tang Y, Zhou Z, Ji E, Lopez GP, Chi EY, Schanze KS, Whitten DG. 2010. Membrane perturbation activity of cationic phenylene ethynylene oligomers and polymers: selectivity against model bacterial and mammalian membranes. Langmuir 26:12509–14.

27. King RD, Lee JC, Morris AL. 1980. Adherence of Candida albicans and other Candida species to mucosal epithelial cells. Infect Immun 27:667–74.

28. Dascier D, Ji E, Parthasarathy A, Schanze KS, Whitten DG. 2012. Efficacy of end-only-functionalized oligo(arylene-ethynylene)s in killing bacterial biofilms. Langmuir 28:11286–90.

29. Zhao X, Pinto MR, Hardison LM, Mwaura J, Müller J, Jiang H, Witker D, Kleiman VD, Reynolds JR, Schanze KS. 2006. Variable band gap poly(arylene ethynylene) conjugated polyelectrolytes. Macromolecules 39:6355–6366.

30. Lowman DW, Greene RR, Bearden DW, Kruppa MD, Pottier M, Monteiro MA, Soldatov D V, Ensley HE, Cheng S-C, Netea MG, Williams DL. 2014. Novel structural features in Candida albicans hyphal glucan provide a basis for differential innate immune recognition of hyphae versus yeast. J Biol Chem 289:3432–43.

31. Wang Y, Schanze K, Chi E, Whitten D. 2013. When worlds collide: Interactions at the interface between biological systems and synthetic cationic conjugated polyelectrolytes and oligomers. Langmuir 8:1–30.

32. Moran G, Coleman D, Sullivan D, Butler G, Hoyer LL, Romani L, Netea MG, Gow NAR, Spellberg B, Fu Y, Ibrahim AS, Jang WS, Edgerton M, Murno C, Richard ML, Brown AJP, Haynes K, Quinn J, Zordan R, Cormack B, Vylkova S, Lorenz MC, Deepu A, Calderone R, Li D, Pfaller MA, Diekema DJ. 2012. Candida and Candidiasis, 2nd ed. ASM Press, Washington DC.

33. Brown JA, Catley BJ. 1992. Monitoring polysaccharide synthesis in Candida albicans. Carbohydr Res 227:195–202.

34. Hong Y, Lam JWY, Tang BZ. 2011. Aggregation-induced emission. Chem Soc Rev

40:5361–88.

35. Donabedian PL, Pham TK, Whitten DG, Chi EY. 2015. Oligo(p-phenylene ethynylene) Electrolytes: A Novel Molecular Scaffold for Optical Tracking of Amyloids. ACS Chem Neurosci 6:1526–35.

36. Fitzpatrick DA, Logue ME, Stajich JE, Butler G. 2006. A fungal phylogeny based on 42 complete genomes derived from supertree and combined gene analysis. BMC Evol Biol 6:99.

37. Tsoni SV, Brown GD. 2008. β-Glucans and Dectin-1. Ann N Y Acad Sci 1143:45–60.

38. Carrion S d. J, Leal SM, Ghannoum MA, Aimanianda V, Latge J-P, Pearlman E. 2013. The RodA Hydrophobin on Aspergillus fumigatus Spores Masks Dectin-1- and Dectin-2-Dependent Responses and Enhances Fungal Survival In Vivo. J Immunol 191:2581–2588.

39. Rappleye CA, Eissenberg LG, Goldman WE. 2007. Histoplasma capsulatum alpha-(1,3)-glucan blocks innate immune recognition by the beta-glucan receptor. Proc Natl Acad Sci U S A 104:1366–70.

40. Wheeler RT, Kombe D, Agarwala SD, Fink GR. 2008. Dynamic, Morphotype-Specific Candida albicans β-Glucan Exposure during Infection and Drug Treatment. PLoS Pathog 4:e1000227.

41. Wheeler RT, Fink GR. 2006. A Drug-Sensitive Genetic Network Masks Fungi from the Immune System. PLoS Pathog 2:e35.

42. Underhill DM, Rossnagle E, Lowell CA, Simmons RM. 2005. Dectin-1 activates Syk tyrosine kinase in a dynamic subset of macrophages for reactive oxygen production. Blood 106:2543–50.

43. Adie EJ, Kalinka S, Smith L, Francis MJ, Marenghi A, Cooper ME, Briggs M, Michael NP, Milligan G, Game S. 2002. A pH-sensitive fluor, CypHer 5, used to monitor agonist-induced G protein-coupled receptor internalization in live cells. Biotechniques 33:1152–4, 1156–7.

44. Adie EJ, Francis MJ, Davies J, Smith L, Marenghi A, Hather C, Hadingham K, Michael NP, Milligan G, Game S. 2003. CypHer 5: a generic approach for measuring the activation and trafficking of G protein-coupled receptors in live cells. Assay Drug Dev Technol 1:251–9.

45. Jamieson DJ, Stephen DW, Terrière EC. 1996. Analysis of the adaptive oxidative stress response of Candida albicans. FEMS Microbiol Lett 138:83–8.

46. Nikolaou E, Agrafioti I, Stumpf M, Quinn J, Stansfield I, Brown AJP. 2009. Phylogenetic diversity of stress signalling pathways in fungi. BMC Evol Biol 9:44.

47. Kaloriti D, Jacobsen M, Yin Z, Patterson M, Tillmann A, Smith D a, Cook E, You T, Grimm MJ, Bohovych I, Grebogi C, Segal BH, Gow N a R, Haynes K, Quinn J, Brown AJP. 2014. Mechanisms Underlying the Exquisite Sensitivity of Candida albicans to Combinatorial Cationic and Oxidative Stress That Enhances the Potent Fungicidal Activity of Phagocytes. MBio 5:1–11.

48. Wilde KNK, Whitten DGD, Canavan HE. 2013. In vitro cytotoxicity of antimicrobial conjugated electrolytes: interactions with mammalian cells. ACS Appl Mater Interfaces 5:9305–11.

49. Sasada M, Johnston RB. 1980. Macrophage microbicidal activity. Correlation between phagocytosis-associated oxidative metabolism and the killing of Candida by macrophages. J Exp Med 152:85–98.

50. Miramón P, Kasper L, Hube B. 2013. Thriving within the host: Candida spp. interactions with phagocytic cells. Med Microbiol Immunol 202:183–95.

51. Bahmed K, Bonaly R, Coulon J. 2003. Relation between cell wall chitin content and susceptibility to amphotericin B in Kluyveromyces, Candida and Schizosaccharomyces species. Res Microbiol 154:215–22.

52. Mesa-Arango AC, Rueda C, Román E, Quintin J, Terrón MC, Luque D, Netea MG, Pla J, Zaragoza O. 2016. Cell wall changes in AmB-resistant strains from Candida tropicalis and relationship with the immune responses elicited by the host. Antimicrob Agents Chemother.

53. Mochon AB, Liu H. 2008. The antimicrobial peptide histatin-5 causes a spatially restricted disruption on the Candida albicans surface, allowing rapid entry of the peptide into the cytoplasm. PLoS Pathog 4:e1000190.

54. Nikawa H, Jin C, Fukushima H, Makihira S, Hamada T. 2001. Antifungal activity of histatin-5 against non-albicans Candida species. Oral Microbiol Immunol 16:250–2.

55. Helmerhorst EJ, Venuleo C, Beri A, Oppenheim FG. 2005. Candida glabrata is unusual with respect to its resistance to cationic antifungal proteins. Yeast 22:705–14.

56. Raman N, Lee M-R, Lynn DM, Palecek SP. 2015. Antifungal Activity of 14-Helical β-Peptides against Planktonic Cells and Biofilms of Candida Species. Pharmaceuticals (Basel) 8:483–503.

57. Briones-Martin-del-Campo M, Orta-Zavalza E, Cañas-Villamar I, Gutiérrez-Escobedo G, Juárez-Cepeda J, Robledo-Márquez K, Arroyo-Helguera O, Castaño I, De Las Peñas A. 2015. The superoxide dismutases of Candida glabrata protect against oxidative damage and are required for lysine biosynthesis, DNA integrity and chronological life survival. Microbiology 161:300–10.

58. Kasper L, Seider K, Hube B. 2015. Intracellular survival of Candida glabrata in macrophages: immune evasion and persistence. FEMS Yeast Res 15:fov042.

59. Lowman D, Ensley H, Williams D. 2005. Introduction to the Chemistry and Immunobiology of Beta-Glucans, p. 1–34. *In* Toxicology of 1 - 3-Beta-Glucans. Informa Healthcare.

60. Young SH, Dong WJ, Jacobs RR. 2000. Observation of a partially opened triple-helix conformation in 1-->3-beta-glucan by fluorescence resonance energy transfer spectroscopy. J Biol Chem 275:11874–9.

61. Horisberger M, Clerc MF. 1988. Ultrastructural localization of anionic sites on the surface of yeast, hyphal and germ-tube forming cells of Candida albicans. Eur J Cell Biol 46:444–52.

62. Cutler JE. 2001. N-glycosylation of yeast, with emphasis on Candida albicans. Med Mycol 39 Suppl 1:75–86.

63. Hall RA, Gow NAR. 2013. Mannosylation in Candida albicans: role in cell wall function and immune recognition. Mol Microbiol 90:1147–61.

Chapter 3

Oligo-phenylene Ethynylene (OPE) Resistance in *Candida glabrata*

3.1 Introduction

Oligo-phenylene ethynylenes (OPEs) are a class of antimicrobial compounds with biocidal mechanisms that include light-induced ROS generation as well as light-independent killing (1, 2). We have found that the phenylene ethynylenes exhibit potent antifungal activity against *Candida albicans* and *Candida parapsilosis*, two medically significant fungal pathogens (3). In contrast, another major *Candida* species pathogen, *Candida glabrata*, displayed intrinsically low susceptibility to OPE dark-killing, relative to *C. ablicans* and *C. parapsilosis* (4).

The intrinsic resistance to oligo-phenylene ethynylene (OPE) seen in *C. glabrata* parallels the species intrinsic resistance to other antifungals like fluconazole (5, 6). *C. glabrata's* intrinsic resistance to drugs has been attributed to the activity of efflux pumps, which pump the drug out of the cytoplasm and reduce the cell's exposure to antifungal medications (7–11). We wanted to determine if efflux pumps play a role in pumping EO-OPE-DABCO from the cell, effectively contributing to OPE resistance in *C. glabrata*. In order to test this hypothesis, we employed a broad spectrum efflux pump inhibitor, clorgyline, to determine whether it was possible to sensitize *C. glabrata* to EO-OPE-DABCO biocidal activity (12).

3.2 Materials & Methods

Strains and media

Type strains - *Candida glabrata* (ATCC, #2001) and *Candida albicans* (ATCC, #MYA-2876), were grown from glycerol stocks, stored at -80 °C. Both type strains were grown in 5 mL filtered yeast extract-peptone-dextrose (YPD) medium (Becton Dickinson), and grown for 16 h to each exponential growth phase at 30 °C, in an orbital incubator at 300 RPM. Such growth conditions yielded yeast at the late log phase. Following a 10 minute centrifugation at 2,900 rcf, the supernatant was replaced with sterile phosphate-buffered saline (PBS), and subsequently vortexed. This washing step is repeated a second time to mitigate cell debris. Cell concentration was then determined using a disposable hemocytometer (INCYTO C-Chip; Fisher Scientific).

Clinical Isolates - Patient specimens (peripheral blood or catheter tips) were processed by Tricore Reference Laboratories (Albuquerque, NM) and identified as *C. glabrata* by FunITS at Charles River. The identified isolates were subcultured on Sabouraud agar slants and provided to the investigators as unique strains. Isolate strains were provided in completely deidentified form according to procedures approved by the University of New Mexico School of Medicine Human Research Protections Office. For biocidal assays, clinical isolates were grown in YPD broth as described above.

S. cerevisiae strains – *S. cerevisiae* AD/pABC3 (control) and *S. cerevisiae* AD/CgCDR1 were gifts from Richard Cannon (University of Otago, New Zealand). Both strains were grown in SD Ura medium at 30 °C for 16 hours to reach exponential growth phase.

Biocidal Testing

Biocidal experiments were carried out in either translucent or opaque 1.5 mL microcentrifuge tubes, at cell concentrations of 5 x 10^6cells/mL in 1X phosphate-buffered

saline (PBS). EO-OPE-DABCO stocks were prepared in sterile deionized water (18.2 MΩ•cm at 25 °C), and contained 0.47% dimethyl sulfoxide (by volume) to improve solubility and minimize aggregate formation. Negative controls contained equal amounts of dimethyl sulfoxide.

Samples were then stained with 5 μM membrane-permeable SYTO 9 and 1 μM membrane-impermeable TO-PRO-3, both of which are nucleic acid stains. After 40 min, samples were evaluated by flow cytometry (FACSCalibur; Becton Dickinson). At least 10,000 events were evaluated in each trial. A heat-killed sample (70 °C for 30 min) was used to identify the fluorescence characteristics of dead cells.

Kinetics Assay - Samples were prepared and stained with SYTO 9 and TO-PRO-3, albeit in the absence of any biocide. After a 40 min staining duration, EO-OPE-DABCO was added (10 μg/mL final concentration); the sample was then vortexed and analyzed by flow cytometry. Every minute, viability data was collected (again, 10,000 events/sample), for a total of 15 minutes. It is important to note that EO-OPE-DABCO was added one sample at a time, so that, in each case, flow cytometry readings could begin within 1 min of the biocide's introduction.

Extended Treatment and *S. cerevisiae* strains - Samples were prepared and stained with SYTO 9 and TO-PRO-3, albeit in the absence of any biocide. After a 40 min staining duration, EO-OPE-DABCO was added (10 μg/mL final concentration); the sample was then vortexed and exposed to the compound in the dark at 15 min, 30 min, and 60 mins respectively for extended treatment and 15 minutes for *S. cerevisiae* strains. Each sample was analyzed by flow cytometry after the lapsed time period.

Clorgyline pretreatment – Prepared samples at cell concentrations of 5 x 10^6cells/mL were pretreated with final concentration of (100, 50, 25, 12.5, and 6.25) mM clorgyline. In the absence of any biocide, samples were incubated for 2h with drug then stained with SYTO 9 and TO-PRO-3 for 40 min. After the lapsed staining period, samples were subject to EO-OPE-DABCO (10 µg/mL final concentration) for 15 min and then analyzed by flow cytometry for an end point viability reading. Clorgyline stocks were prepared in dimethyl sulfoxide. Negative controls contained equal amounts of dimethyl sulfoxide.

Multi-photon microscopy

Sample preparation – *C. glabrata*, *C. albicans*, and clorgyline pretreated *C. glabrata* cells were seeded on glass-bottomed MatTek dishes (MatTek Corp., Ashland, MA) at a density of 10^5 cells/plate in 1X phosphate-buffered saline (PBS),

Two-photon Fluorescence Imaging – Microscopy readings began within 1 min of EO-OPE-DABCO introduction (1 µg/mL final concentration). EO-OPE-DABCO fluorescent entry was monitored using multi-photon excitation on Zeiss LSM 510 Confocal Microscope (Zeiss, Oberkochen, Germany) equipped with 63X oil immersion objective. Samples were excited with a 20mW, 710nm laser operated at 0.5% power. A 390/40nm BrightLine Bandpass Filter (25mm) was used to detect OPE emission. Control experiments were conducted to minimize cellular auto fluorescence, which was not seen until laser power was increased to 6%.

Quantitative real-time RT-PCR

This protocol was adapted from Sanguinetti et al. 2005. Total RNA was extracted from *C. glabrata* (ATCC2001) and TRL026 cultures grown to the mid-exponential phase (optical

density at 600 nm [OD_{600}], approximately 0.6) with an RNAeasy Protect mini kit (Qiagen, Hilden, Germany), according to the instructions of the manufacturer, by mechanical disruption of the cells with glass beads and an RNase-free DNase treatment step. RNA integrity was assessed by determination of the OD_{260}/OD_{280} absorption ratio, and the integrity was considered maintained if the ratio was >1.95. Quantitative expression of the CgCDR1 gene was performed by real-time RT-PCR with a Lightcyler 96 system (Roche Diagnostics, Indianapolis, IN).

RT-PCR was performed with a 50-µl volume containing the following reagents: 25 µl of the Platinum Quantitative RT-PCR ThermoScript reaction mixture (Invitrogen Inc., Milan, Italy), 1.5 U of the ThermoScript Plus/Platinum *Taq* mixture (Invitrogen), each primer pair and the Taqman probe at a concentration of 5 µM, 5 µl of total RNA sample (5, 10, 25, 50, and 100 ng), and distilled water up to the final volume.

Samples were subjected to an initial step at 52°C for 45 min for RT; 94°C for 5 min to inactivate the ThermoScript Plus reverse transcriptase and to activate the Platinum *Taq* polymerase; and 50 cycles, each of which consisted of 15 s at 94°C and 1 min at 59°C. Fluorescence data were collected during the 59°C annealing and extension step and were analyzed with the i-Cycler iQ software. Each reaction was run in duplicate.

3.3 Results

Recent research has explored the use of phenylene ethynylenes as novel antifungals*, Candida glabrata* displayed intrinsically low-susceptibility to oligo-phenylene ethynylene (OPE) as comparted to *C. ablicans* and *C. parapsilosis* (4). A series of experiments were conducted to elucidate the mechanism of OPE-resistance in *C. glabrata.* The mechanism

of action for EO-OPE-DABCO differs depending on the presence or absence of light. The subsequent studies were performed in dark; the compound was not subject to light irradiation.

It was important to replicate previously published results and validate that EO-OPE-DABCO was indeed more effective against type strain *C. albicans* (SC5314) than *C. glabrata* (ATCC2001).

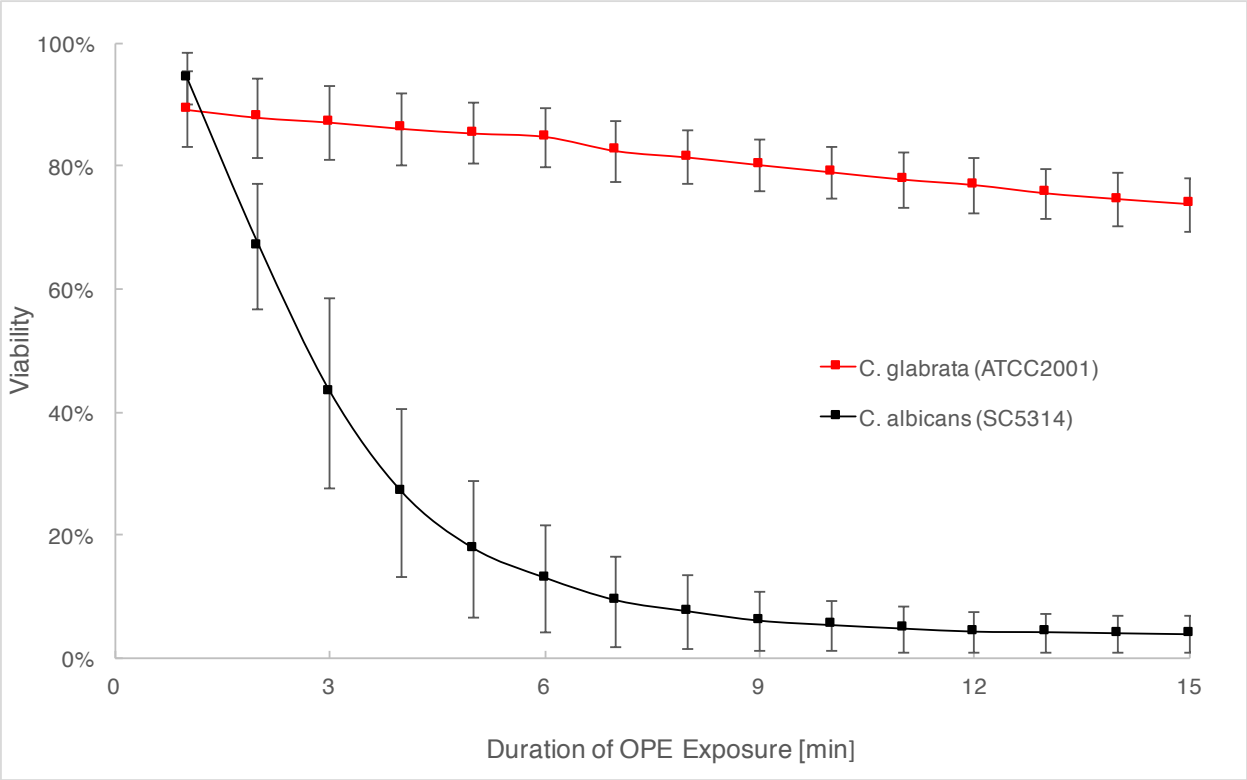

Figure 1: Viability of *C. albicans* and *C. glabrata* in the presence of 10 µg/mL EO-OPE-DABCO in the dark.

Figure 1 shows that *C. glabrata* is less susceptible to EO-OPE-DABCO after 15 minutes of exposure. The cells were stained with SYTO 9 and TO-PRO-3 before the introduction of EO-OPE-DABCO. Taking a flow cytometry dual-fluorescent measurement of 10,000 events every minute allowed for real-time reporting of OPE-induced membrane perturbation. These results were consistent with previously published results that showed EO-OPE-DABCO biocidal activity is more effective against *C. albicans*.

Using a modified biocidal assay, cell exposure to EO-OPE-DABCO was varied to determine the degree of OPE resistance *C. glabrata* displayed. In addition to the custom 15 minute viability reading, readings after 30 min and 60 min OPE exposure were tested. Increasing cell exposure to the compound did not increase *C. glabrata* susceptibility relative to *C. albicans* (SC5314), as shown in Fig. 2.

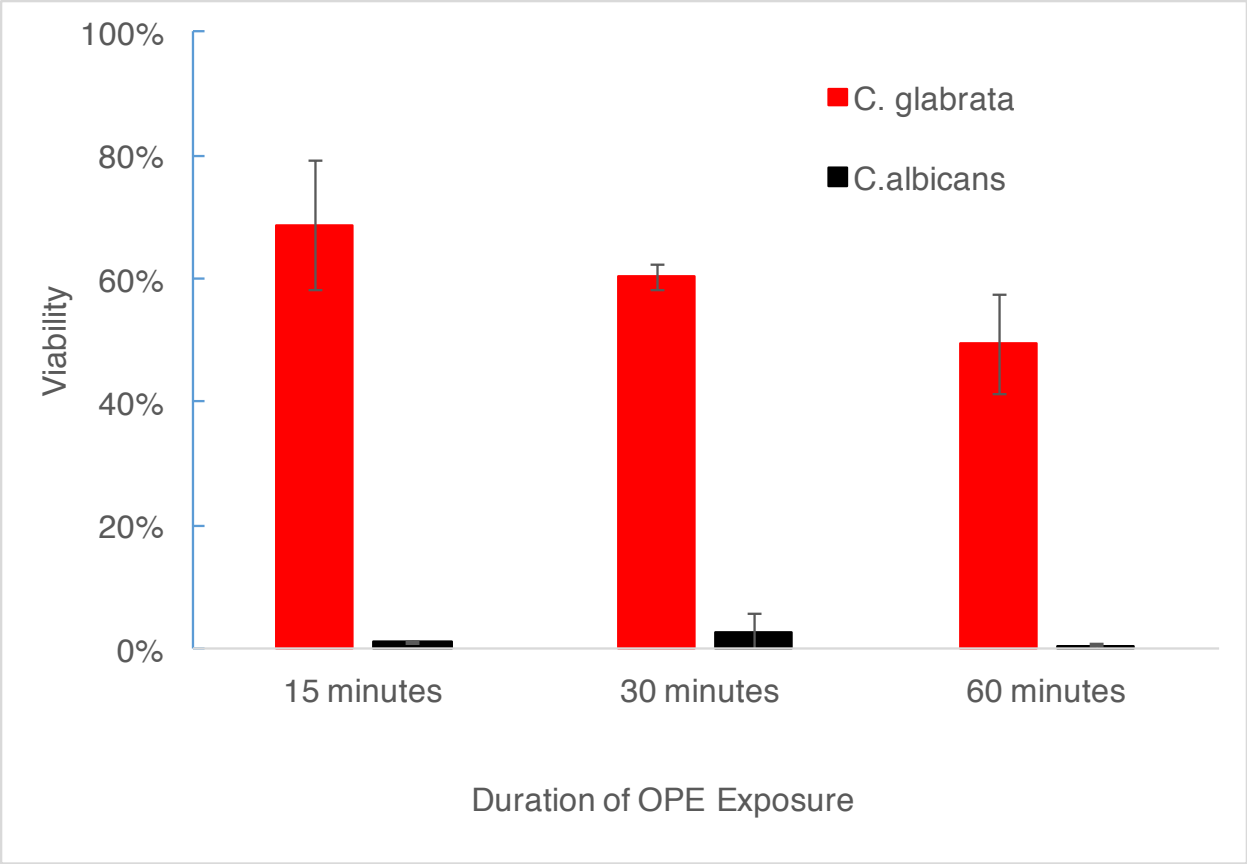

Figure 2: Viability of *C. albicans* and *C. glabrata* after treatment with of 10 µg/mL EO-OPE-DABCO in the dark at 15 min, 30 min, and 60 min.

Additionally, Figure 2 illustrates that after increasing exposure time four fold, EO-OPE-DABCO was unable to induce complete *C. glabrata* cell death.

While EO-OPE-DABCO was highly effective at killing the standard type strain *C. albicans* (SC5314) and *C. albicans* clinical isolates, we sought to determine whether *C. glabrata* clinical isolates were also less susceptible to OPE. From an extensive clinical isolate library, six *C. glabrata* clinical isolates were surveyed for their susceptibility to 10 µg/mL

EO-OPE-DABCO in the dark. The susceptibility of clinical isolates was gauged relative to that of *C. glabrata* ATCC2001, as shown in Fig. 3.

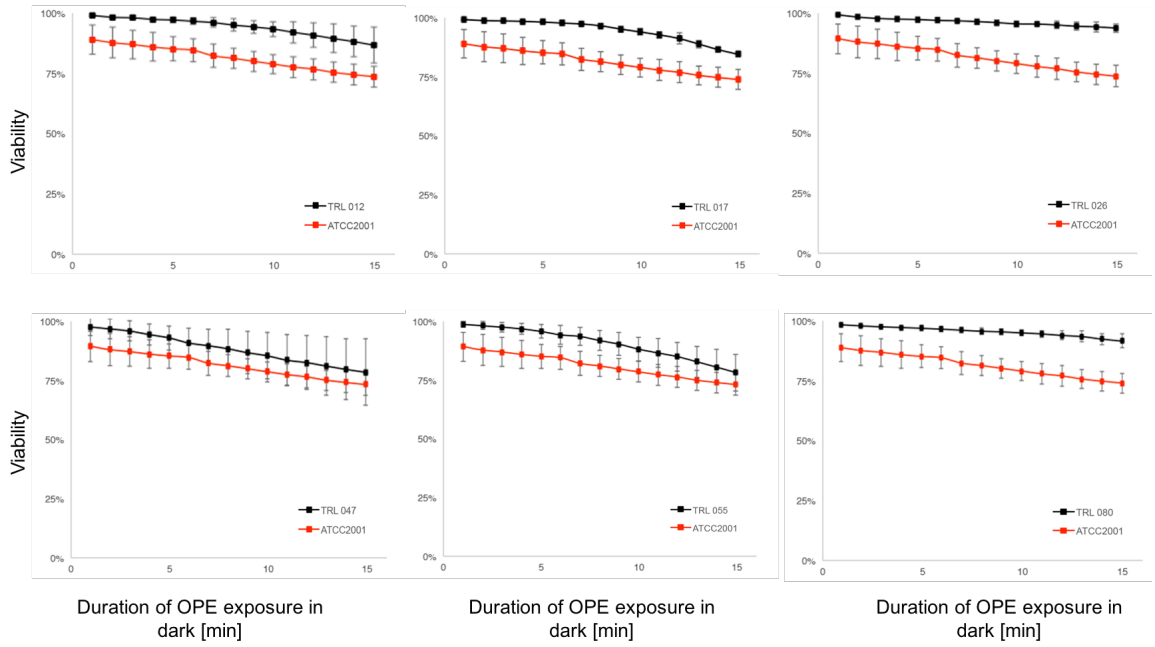

Figure 3: Susceptibility of various *C. glabrata* clinical isolates to 10 µg/mL EO-OPE-DABCO in the dark. Lab strain ATCC2001 is shown for reference in all cases. Strains prefixed "TRL" are recent (circa 2015) clinical isolates obtained as described in *Materials and Methods*.

These results consistently show that *C. glabrata* is able to withstand the biocidal activity of EO-OPE-DABCO as compared to other tested pathogens (13–17).

The intrinsic resistance to oligo-phenylene ethynylene (OPE) seen in *C. glabrata* parallels the species intrinsic resistance to other antifungals, like fluconazole, which can be mediated by efflux pumps. We employed a broad spectrum efflux pump inhibitor,

clorgyline (12), to determine whether it was possible to sensitize *C. glabrata* to EO-OPE-DABCO biocidal activity. Before exposure to EO-OPE-DABCO, cells were incubated with clorgyline at varying concentrations. It was important to determine whether the effect of clorgyline was synergistic or additive. Using the proper dimethyl sulfoxide and clorgyline controls, a synergistic index was calculated. The index was calculated using the equation (Fig. 4). A value of one would indicate an additive effect of both compounds. Figure 4A illustrates the effect various concentrations of clorgyline treatment had on OPE killing. At 25 ug/mL, clorgyline was able to most effectively sensitize yeast *C. glabrata* cells to OPE killing, the calculated synergistic index at this concentration was 2.24.

[A]

$$I = \frac{Kill_{[OPE+clorgyline]}}{Kill_{[OPE]} + Kill_{[clorgyline]}}$$

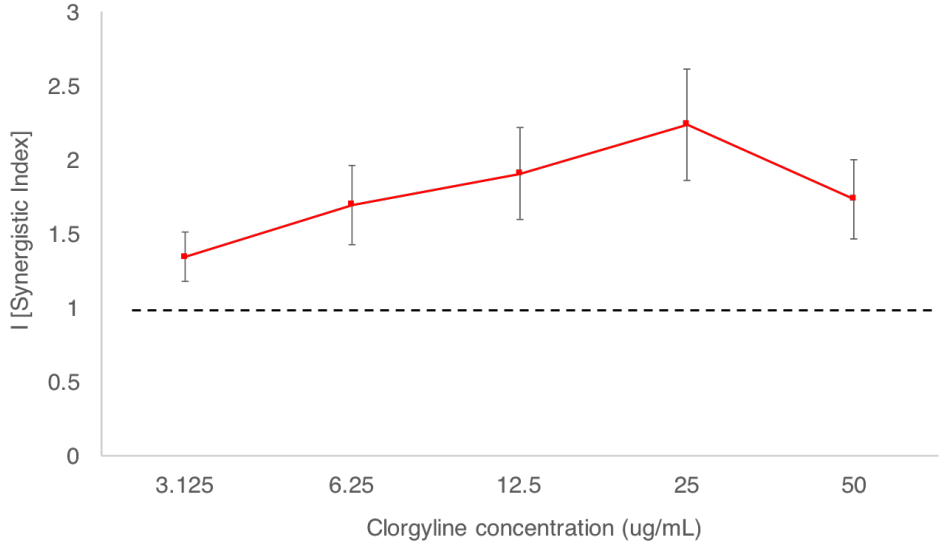

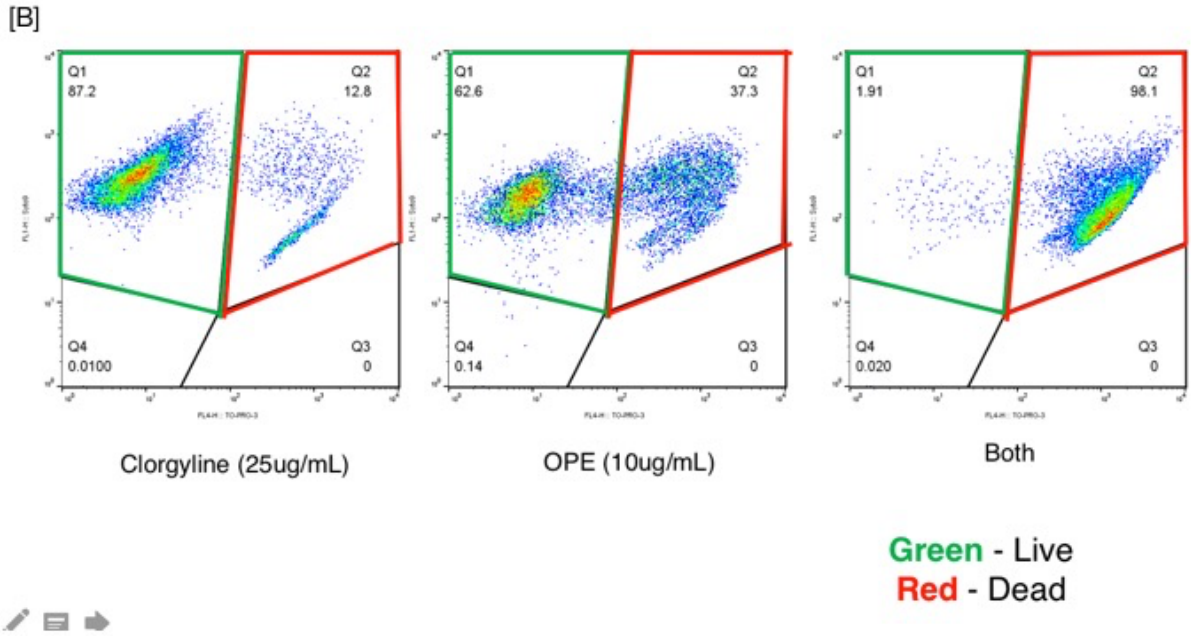

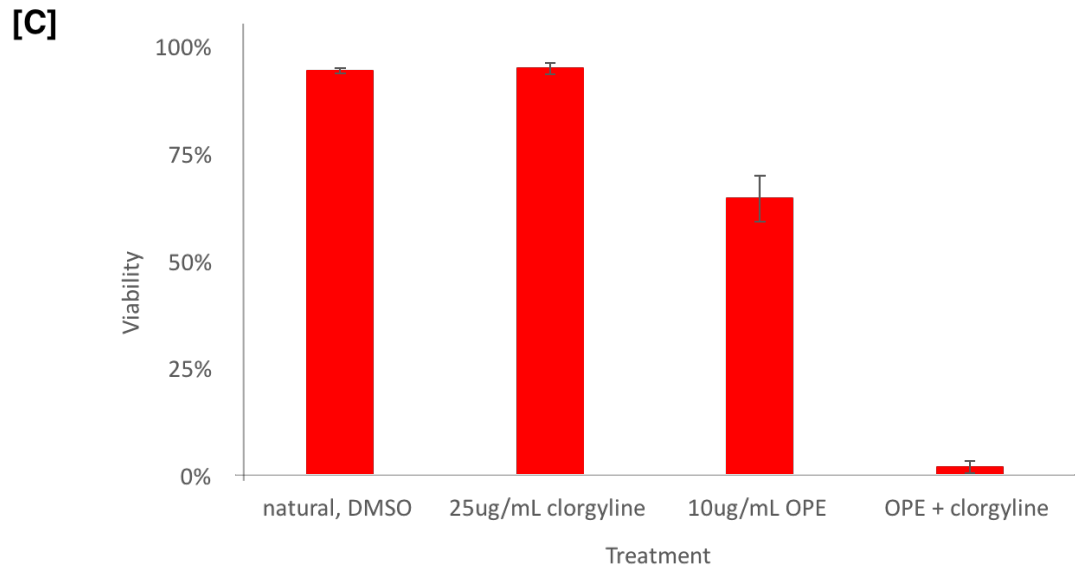

Figure 4[A]. Synergistic effects of clorgyline at varying concentrations when *C. glabrata* (ATCC2001) is treated with 10 µg/mL EO-OPE-DABCO. The synergistic index was calculated using the equation above, a value of 1 indicates a purely additive killing effect of clorgyline and EO-OPE-DABCO. **Figure 4[B].** Flow cytometry readings for

three treatments are shown (25ug/mL clorgyline, 10ug/mL OPE, and combined treatment of 25ug/mL clorgyline and 10ug/mL OPE). The events in the green gate are live cells and the events in the red gate are dead cells. **Figure 4[C].** The viability of *C. glabrata* (ATCC2001) cells after each specified treatment is shown. Treating cells with 25ug/mL clorgyline and then 10ug/mL OPE induced complete cell death.

At this concentration cell death by clorgyline was simultaneously minimized while cell death by OPE was maximized. This effect is most clearly illustrated in Figure 4B. The flow cytometry contour plots illustrate the synergistic effect between 25 ug/mL clorgyline with 10 ug/mL EO-OPE-DABCO. The flow cytometry dual-fluorescent assay, shows that most events after pretreatment with 25 ug/mL clorgyline appeared in the dead gate, as measured by TO-PRO-3 perturbation (Fig. 4B). At this concentration of clorgyline, *C. glabrata* cells are sensitized to OPE killing and almost complete cell death is induced (Fig. 4C).

EO-OPE-DABCO is fluorescent when excited with 355nm light (1, 18, 2). This characteristic allowed us the capacity to directly measure cytoplasmic concentration of OPE in the yeast cells using two-photon microscopy (Figure 5). It was important to observe cytoplasmic entry of the compounds in order to understand the role efflux pumps might play in reducing sensitivity to EO-OPE-DABCO in *C. glabrata* on the cellular level. We hypothesized that there would be lower cytoplasmic concentration of EO-OPE-DABCO in *C. glabrata* relative to *C. albicans*. Subsequently we expected to observe an increase in cytoplasmic concentration of OPE in *C. glabrata* after application of clorgyline.

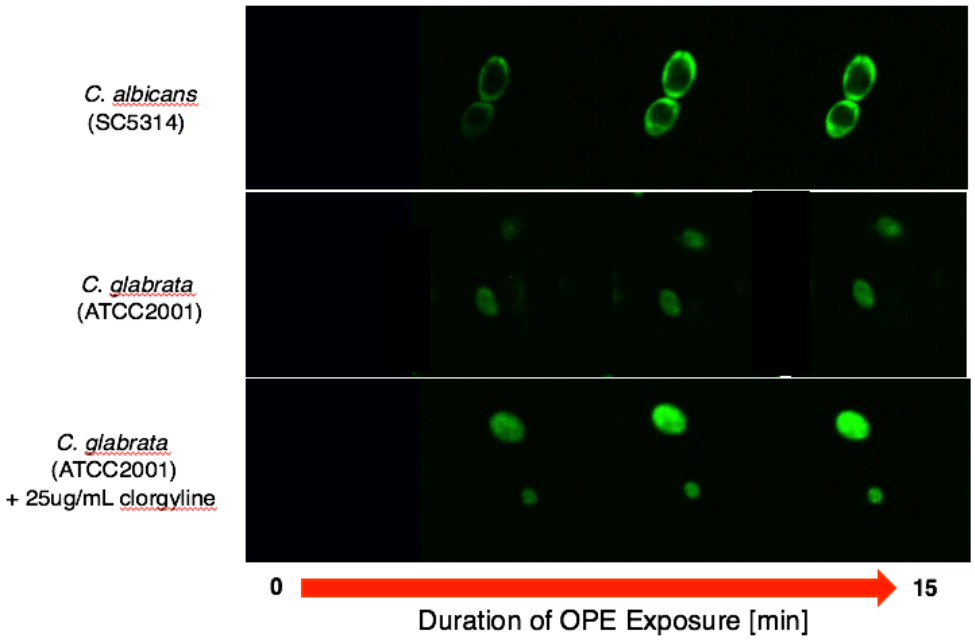

Figure 5. Two-photon microscopy images show the intracellular accumulation of 10 µg/mL EO-OPE-DABCO over the course of 15 minutes.

Using two-photon imaging provided a way to fluorescently track the kinetic entry of OPE into the yeast cells through the 15 minute time course. The images taken at different time points show the accumulation of OPE in the cell as depicted by increasing fluorescence (Figure 5).

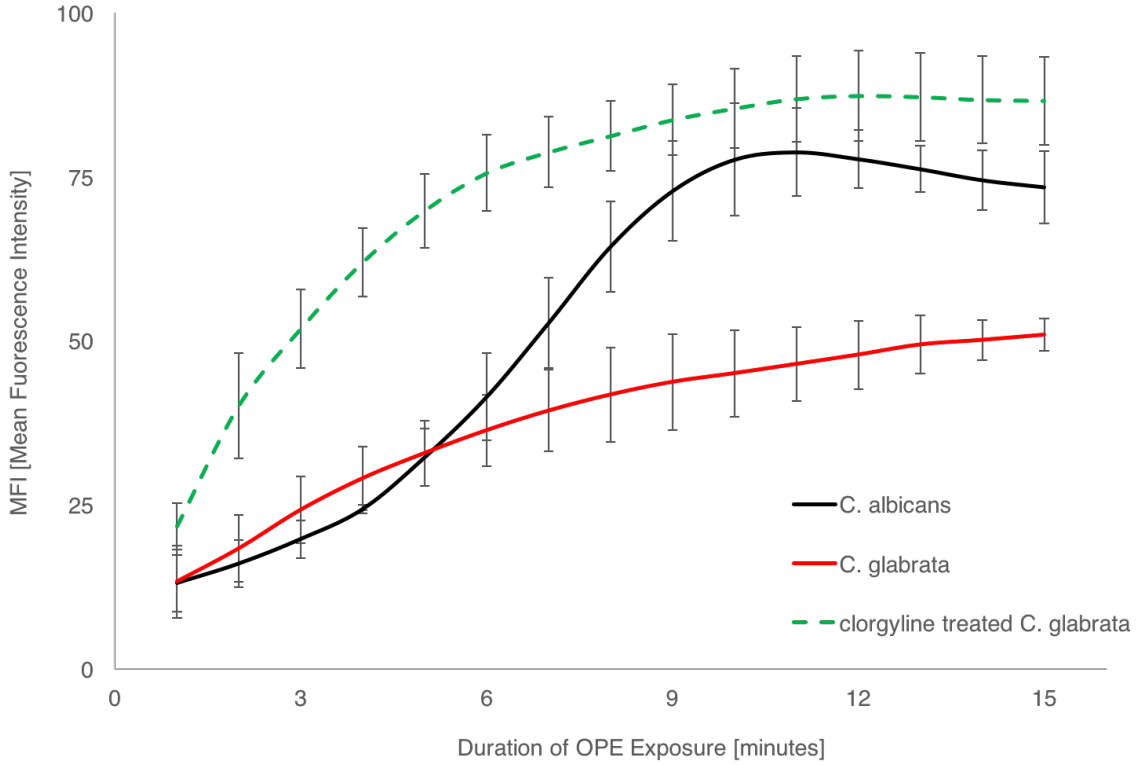

Figure 6. The OPE entry kinetics were monitored using two-photon microscopy in *C. albicans* (SC5314) cells, *C. glabrata* (ATCC2001) cells, and 25 ug/mL clorgyline pretreated *C. glabrata* (ATCC2001) cells over the course of 15 mintues.

We hypothesized that there would be lower cytoplasmic concentration of EO-OPE-DABCO in *C. glabrata* relative to *C. albicans*. The compound was introduced to the yeast cells within in a minute of imaging. The kinetic entry of OPE was tracked by measuring mean fluorescent intensity every minute across 60 cells. We observed slower accumulation of OPE in *C. glabrata* (Figure 5 and Figure 6). Additionally, pretreatment of *C. glabrata* with clorgyline increased OPE accumulation closer to *C. albicans'* levels. Both

flow cytometric assays and two-photon imaging suggest that efflux pumps might play a role in regulating OPE-resitance in *C. glabrata*.

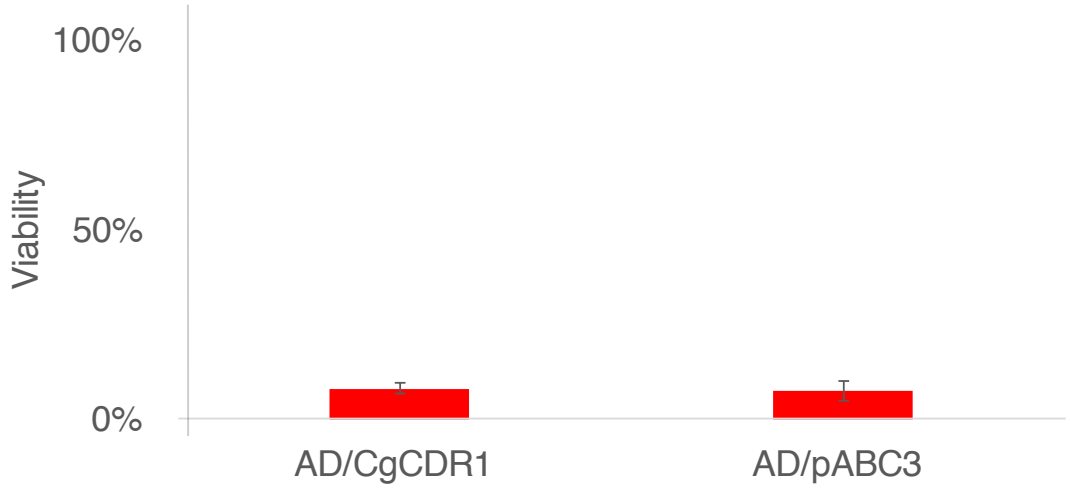

Figure 7. Treatment of *Saccharomyces cerevisiae* AD/pABC3 and AD/CgCDR1 mutant strains with 10 µg/mL EO-OPE-DABCO in the dark.

The effect of clorgyline to enhance OPE killing led us to question what specific efflux pump was being targeted. Clorgyline has been identified as a broad spectrum pump inhibitor and was specifically able to reverse fluconazole-resistance in a *S. cerevisiae* mutant that overly expressed efflux pump *CgCDR1.* We tested the *S. cerevisiae* AD/pABC3 (control) and *S. cerevisiae* AD/CgCDR1 (over-expression) strains to see if the over-expression of CgCDR1 conferred OPE-resistance. When treated with 10ug/mL EO-OPE-DABCO, the *S. cerevisiae* AD/CgCDR1 was no more resistant to the compound than the control *S. cerevisiae* AD/pABC3 or *C. glabrata* (ATCC2001). These results

indicate that clorgyline does not act on CgCDR1 in a manner that contributes to OPE-resistance.

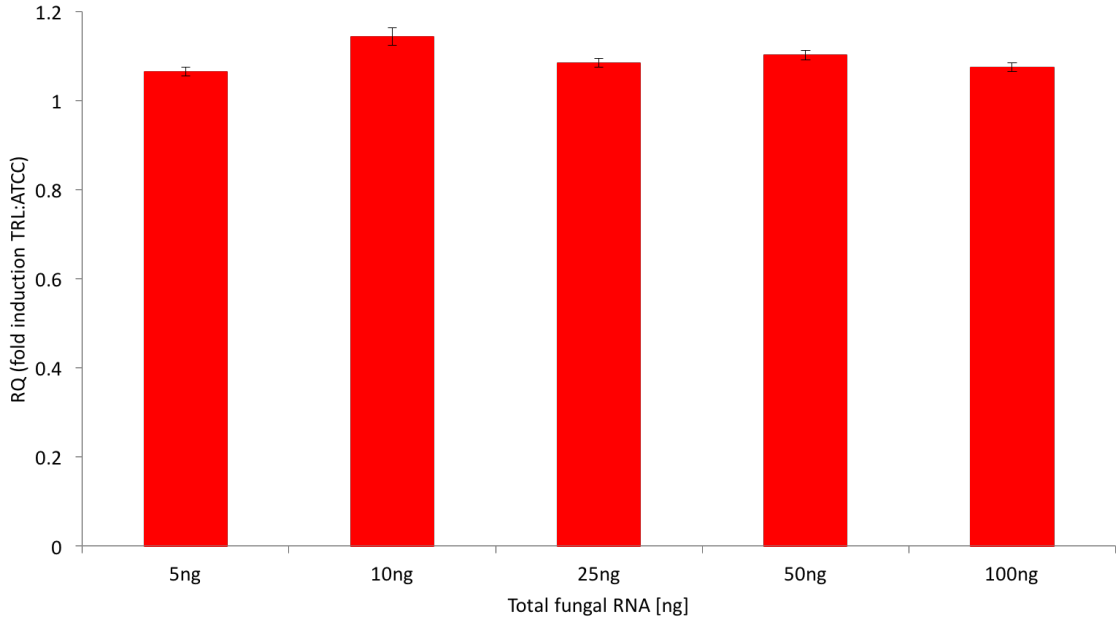

Figure 8. Fold induction difference between TRL 026 and ATCC 2001 for CgCDR1 for different amounts of extract RNA. The fold induction difference does exceed a value of 1.10.

Consistent with these results, we found no upregulation of CgCDR1 at the message level in one of the more resistant isolates, TRL026, as compare to the type strain (ATCC2001). This was determined by qRT-PCR (Figure 8).

3.4 Discussion

Despite the effective biocidal activity of EO-OPE-DABCO against *C. albicans* in the dark, *C. glabrata* possess an intrinsic resistance to the compound (4). The light-independent mechanism of killing is not effective enough to induce complete cell death of *C. glabrata*

even after prolonged exposure to the compound (Figure 1 and Figure 2). The intrinsic resistance to OPE seen in *C. glabrata* is unique in comparison to other *Candida* species tested, but consistent with its response to other antifungals. Specifically, *C. glabrata* possess significant healthcare threats because of its characteristic intrinsic and acquired resistance to common antifungals such as azoles (19–21).

While the inhibitory effects of clorgyline are considered broad spectrum, our data suggests that CgCDR1, a major efflux pump, is not implicated in OPE sensitivity when heterologously expressed in *S. cerevisiae* (8, 12, 22). The target of clorgyline in sensitizing *C. glabrata* to OPE killing needs to be further studied. Clorgyline was initially marketed as an antidepressant, inhibiting cytochrome P450 monoamine oxidase A, a member of the flavin monoxidase family (23). Yeast species are known to have members of this family of enzymes. In *C. glabrata*, a well characterized cytochrome P450 is lanoserol 14-alpha-demethylase encoded by ERG11, the target of fluconazole. ERG11 is known be involved in ergosterol synthesis and ergosterol content affects membrane fluidity in fungi (24). Consequently, clorgyline might act on this P450 enzyme affecting the plasma membrane environment and other membrane proteins such as efflux pumps.

The differential OPE sensitivity between *Candida* species might be attributed to lipid composition. Previous work has shown that drug resistance can arise from an altered membrane sterol pattern in yeast (25, 26). Similarly, the lipid composition in *Candida glabrata* might better facilitate membrane perturbation by the quaternary ammonium side groups on EO-OPE-DABCO. Model membranes, mimicking those of bacterial membranes and mammalian membranes showed significant membrane perturbation by OPE against only against bacterial mimic membranes (27).

In addition, our results indicate that *C. glabrata* is not killed much more by extending the EO-OPE-DABCO dark treatment significantly beyond 15minutes (Figure 2). The target of EO-OPE-DABCO membrane disruption could be intracellular organelles, like the vacuole and mitochondria. Disruption of these membranes and their associated proton gradients would be regulated by intracellular EO-OPE-DABCO concentration, which is in turn related by the balance between diffusion of EO-OPE-DABCO into the cell and pumping of EO-OPE-DABCO back out. Our results indicate that when we treat the cells with clorgyline, killing by EO-OPE-DABCO is increased and intracellular concentration is increased (Figure 4 and 6). Increasing intracellular concentration targets intracellular organelles and results in the loss of membrane integrity measure by TO-PRO-3 uptake. Future work would involve checking whether treatment with EO-OPE-DABCO damages the ability of vacuolar and/or mitochondrial membranes to maintain their proton gradient. We would argue that intracellular membranes may be the actual target of EO-OPE-DABCO. It is suggestive that yeast regulates its susceptibility to the antimicrobial by protecting intracellular membrane by keeping the intracellular antimicrobial concentration low enough to protect plasma membrane integrity.

Understanding the mechanisms of OPE resistance of *C. glabrata* is clinically significant because they will allow the development of novel strategies to prevent and treat infection by this emerging pathogen. While PE's possess a dual-mechanism of action, the light-independent mechanism of killing of OPE is more practical for clinical use. The application of clorgyline as an avenue to reverse OPE-resistance in *C. glabrata* confers a clinical benefit for the use of EO-OPE-DABCO as a future antifungal.

References

1. Hill EH, Pappas HC, Whitten DG. 2014. Activating the antimicrobial activity of an anionic singlet-oxygen sensitizer through surfactant complexation. Langmuir 30:5052–6.
2. Zhao, Xiaoyong, Pinto, Maurico R., Hardison, Lindsay M., Mwaura, Jeremiah, Muller, Juergen, Jian, Hui, Witker, David, Kleiman, Valeria D., Reynolds, John R., Schanze KS. 2006. Variable Band Gap Poly(arylene ethynylene) Conjugated Polyelectrolytes. Macromolecules 39:6355–6366.
3. Wingard JR. 1995. Importance of Candida Species Other Than Candida-Albicans as Pathogens in Oncology Patients. Clin Infect Dis 20:115–125.
4. Pappas HC, Sylejmani R, Graus MS, Donabedian PL, Whitten DG, Neumann K. 2016. Antifungal Properties of Cationic Phenylene Ethynylenes and Their Impact on -Glucan Exposure. Antimicrob Agents Chemother 60:4519–4529.
5. Richter SS, Galask RP, Messer SA, Hollis RJ, Diekema DJ, Pfaller MA. 2005. Antifungal susceptibilities of Candida species causing vulvovaginitis and epidemiology of recurrent cases. J Clin Microbiol 43:2155–2162.
6. Pfaller MA, Diekema DJ. 2007. Epidemiology of invasive candidiasis: A persistent public health problem. Clin Microbiol Rev 20:133–163.
7. Cannon RD, Lamping E, Holmes AR, Niimi K, Baret P V., Keniya M V., Tanabe K, Niimi M, Goffeau A, Monk BC. 2009. Efflux-mediated antifungal drug resistance. Clin Microbiol Rev 22:291–321.
8. Sanguinetti M, Posteraro B, Fiori B, Ranno S, Torelli R, Fadda G. 2005. Mechanisms of Azole Resistance in Clinical Isolates of Candida glabrata Collected during a Hospital Survey of Antifungal Resistance Mechanisms of Azole Resistance in Clinical Isolates of Candida glabrata Collected during a Hospital Survey of Antifungal Re. Society 49:668–679.
9. Perea S, López-ribot JL, Kirkpatrick WR, Mcatee RK, Santillán RA, Marti M, Calabrese D, Sanglard D, Thomas F. 2001. Prevalence of Molecular Mechanisms of Resistance to Azole Antifungal Agents in Candida albicans Strains Displaying High-Level Fluconazole Resistance Isolated from Human Immunodeficiency Virus-Infected Patients Prevalence of Molecular Mechanisms of Resista. Antimicrob Agents Chemother 45:2676–2684.
10. White TC, Marr KA. 1998. Clinical , Cellular , and Molecular Factors That Contribute to Antifungal Drug Resistance. Clin Microbology Rev 11:382–402.
11. Ferrari S, Ischer F, Calabrese D, Posteraro B, Sanguinetti M, Fadda G, Rohde B, Bauser C, Bader O, Sanglard D. 2009. Gain of function mutations in CgPDR1 of

Candida glabrata not only mediate antifungal resistance but also enhance virulence. PLoS Pathog 5.

12. Holmes AR, Keniya M V., Ivnitski-Steele I, Monk BC, Lamping E, Sklar LA, Cannon RD. 2012. The monoamine oxidase A inhibitor clorgyline is a broad-spectrum inhibitor of fungal ABC and MFS transporter efflux pump activities which reverses the azole resistance of Candida albicans and Candida glabrata clinical isolates. Antimicrob Agents Chemother 56:1508–1515.
13. Wang Y, Chi EY, Natvig DO, Schanze KS, Whitten DG. 2013. Antimicrobial activity of cationic conjugated polyelectrolytes and oligomers against Saccharomyces cerevisiae vegetative cells and ascospores. ACS Appl Mater Interfaces 5:4555–61.
14. Lu L, Rininsland FH, Wittenburg SK, Achyuthan KE, McBranch DW, Whitten DG. 2005. Biocidal activity of a light-absorbing fluorescent conjugated polyelectrolyte. Langmuir 21:10154–10159.
15. Chemburu S, Corbitt TS, Ista LK, Ji E, Fulghum J, Lopez GP, Ogawa K, Schanze KS, Whitten DG. 2008. Light-induced biocidal action of conjugated polyelectrolytes supported on colloids. Langmuir 24:11053–11062.
16. Corbitt TS, Sommer JR, Chemburu S, Ogawa K, Ista LK, Lopez GP, Whitten DG, Schanze KS. 2009. Conjugated polyelectrolyte capsules: Light-activated antimicrobial micro “roach Motels.” ACS Appl Mater Interfaces 1:48–52.
17. Wang Y, Canady TD, Zhou Z, Tang Y, Price DN, Bear DG, Chi EY, Schanze KS, Whitten DG. 2011. Cationic phenylene ethynylene polymers and oligomers exhibit efficient antiviral activity. ACS Appl Mater Interfaces 3:2209–2214.
18. Zhou Z, Corbitt TS, Parthasarathy A, Tang Y, Ista LF, Schanze KS, Whitten DG. 2010. “End-Only” Functionalized Oligo(phenylene ethynylene)s: Synthesis, Photophysical and Biocidal Activity. J Phys Chem Lett 1:3207–3212.
19. Safdar A, Chaturvedi V, Koll BS, Larone DH, Perlin DS, Armstrong D. 2002. Prospective , Multicenter Surveillance Study of Candida glabrata : Fluconazole and Itraconazole Susceptibility Profiles in Bloodstream , Invasive , and Colonizing Strains and Differences between Isolates from Three Urban Teaching Hospitals in New York City (Candida Susceptibility Trends Study , 1998 to 1999) 46:3268–3272.
20. Alexander BD, Johnson MD, Pfeiffer CD, Jiménez-ortigosa C, Catania J, Booker R, Castanheira M, Messer SA, Perlin DS, Pfaller MA. 2013. Increasing Echinocandin Resistance in Candida glabrata : Clinical Failure Correlates With Presence of FKS Mutations and Elevated Minimum Inhibitory Concentrations 56:1724–1732.

21. Kanafani ZA, Perfect JR. 2008. Resistance to Antifungal Agents : Mechanisms and Clinical Impact 46.

22. Sanglard D, Ischer F, Bille J. 2001. Role of ATP-Binding-Cassette Transporter Genes in High-Frequency Acquisition of Resistance to Azole Antifungals in Candida glabrata 45:1174–1183.

23. Vallon O. 2000. New sequence motifs in flavoproteins: Evidence for common ancestry and tools to predict structure. Proteins Struct Funct Genet 38:95–114.

24. Odds, FC;Brown, AJ;Gow N. 2003. Antifungal agents: mechanism of action. Trends Microbiol 11:272–279.

25. Mishra NN, Prasad T, Sharma N, Gupta DK. 2008. MEMBRANE FLUIDITY AND LIPID COMPOSITION OF FLUCONAZOLE RESISTANT AND SUSCEPTIBLE STRAINS OF CANDIDA ALBICANS ISOLATED FROM DIABETIC PATIENTS 219–225.

26. Prasad T, Chandra A, Mukhopadhyay CK, Prasad R. 2006. Unexpected Link between Iron and Drug Resistance of Candida spp .: Iron Depletion Enhances Membrane Fluidity and Drug Diffusion , Leading to Drug-Susceptible Cells □ 50:3597–3606.

27. Wang Y, Tang Y, Zhou Z, Ji E, Lopez GP, Chi EY, Schanze KS, Whitten DG. 2010. Membrane perturbation activity of cationic phenylene ethynylene oligomers and polymers: selectivity against model bacterial and mammalian membranes. Langmuir 26:12509–12514.

Chapter 4

Conclusions and Recommendations for Future Work

4.1 Efficacy of PPE-DABCO and EO-OPE-DABCO against *Candida* spp. hyphae and biofilms

In Chapter 2, the efficacy of PPE-DABCO and EO-OPE-DABCO as antifungals was examined. These experiments were however limited to yeast cells. It is important to further extend testing these compounds against *C. albicans* hyphae and biofilms, because most candidiasis infections persist as biofilms (1–4) . Preliminary studies have been done assessing the effectiveness of EO-OPE-DABCO as *C. albicans* hyphae (Figure 1). Using SYTO9 and TO-PRO-3 viability staining (Chapter 1), the fluorescent confocal images show that OPE is able effective against *C. albicans* hyphae as assessed by TO-PRO-3 uptake (red). The quantification of total hyphal cell death is something that needs further work.

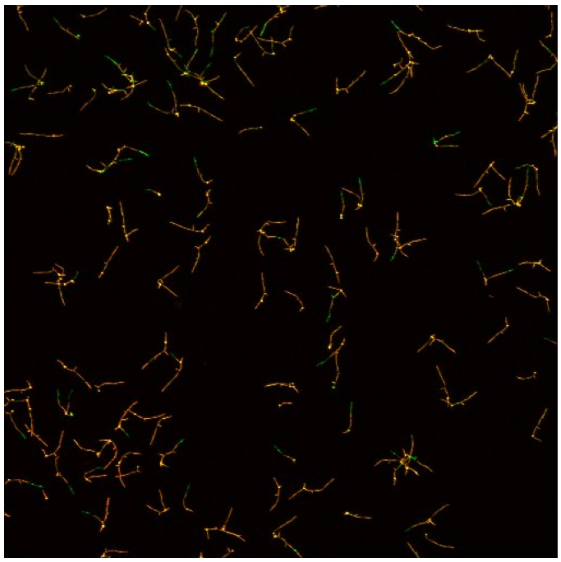

10ug/mL OPE in the dark

Green (Syto9) – Live
Red (TO-PRO-3) – Dead

Figure 9: *C. albicans* hyphae treatment with 10ug/mL of EO-OPE-DABCO in the dark for 60 minutes

New experiments will require treating *C. albicans* hyphae and biofilms with both PPE-DABCO and EO-OPE-DABCO in the dark and when irradiated by the appropriate wavelength. Viability would be assessed through TO-PRO-3 uptake. I would expect to see more efficient cell killing with OPE because of its dual capabilities to kill effectively in the dark and in the light. Since, PPE-DABCO is more likely to associate with components in extracellular matrix such as B-glucan (Chapter 1, Figure 6), I would expect to see less efficient killing (5). In turn, PPE-DABCO might get stuck in the biofilm matrix before being able to induce cell damage.

4.2 Determining efflux pumps involved in OPE-resistance in *Candida glabrata*

In Chapter 3, the intrinsic OPE-resistance seen in *C. glabrata* was investigated. The experiments performed were part of an inhibitory study that suggest clorgyline is effective at improving the efficacy of OPE against *C. glabrata*. There is future work needed to determine the mechanism behind this resistance in *C. glabrata.* A major efflux pump, CgCDR1, seems to not impact OPE sensitivity when heterologously expressed in *S. cerevisiae.* While this pump cannot be implicated in OPE-resistance in *C. glabrata*, other pumps related to multidrug resistance in *C. glabrata* such as CgCdr2 (Pdh1), and CgSnq2 have yet to be tested (6, 7). As a broad-spectrum pump inhibitor, it is possible that clorgyline could be acting on these pumps. Testing *S. cerevisiae* strains that over-express these pumps and performing qRT-PCR on especially OPE resistant clinical isolates might yield insight on how *C. glabrata* is able to resist OPE killing on a molecular level. Additionally, clorgyline effects both ABC and MFS transporters, which have different

mechanisms of pumping (8). There is little known about MFS transporters in *C. glabrata* and their impact on drug resistance. With further studies, it is possible that OPE resistance seen in *C. glabrata* could also be facilitated by MFS transporters as well.

4.3 Investigating clorgyline's mechanism of action in *Candida glabrata*

The mechanism of action of clorgyline might involve more than efflux regulation but also the regulation of membrane lipid composition. If clorgyline is inhibiting ERG11, a cytochrome P450 in *C. glabrata* (7, 9), it could be reducing ergosterol concentration in the membrane, but not enough to produce notable antifungal effects. This would be similar to the effect of fluconazole on ERG11. It could also be indirectly targeting the sterol transporter CgAUS1 that has shown to protect cells against azoles in the presence of serum. CgAUS1 gene product functions as a sterol transporter that ameliorates the growth inhibition caused by the loss of ERG9 expression or fluconazole-mediated inhibition of Erg11p (10). While efflux regulation is part of OPE-resistance in *C. glabrata,* the alternative hypothesis might be clorgyline increases susceptibility of *C. glabrata* to OPE by lowering the plasma membrane ergosterol content, which makes the membrane more susceptible to disruption by OPE. One direct approach to examine this would be to make vesicles from pure phospholipids and ergosterol, vary the amount of ergosterol and see if it changes sensitivity to OPE.

4.4 Potential applications of phenylene ethynylenes

Some anti-fungal medical applications envisioned for phenylene ethynylenes concern treatment of medical devices or topical applications in wound care. For instance, prevention of catheter infections using improved antimicrobial materials or preventive device treatment regimens could save lives, improve quality of life and reduce costs

associated with treating catheter-associated infections. However, providing light to activate phenylene ethynylenes in the catheter context is an important challenge. First, we showed that EO-OPE-DABCO has strong biocidal activity against *C. albicans,* even without light activation, so it is possible that this compound could be used in antifungal lock solutions even without illumination. Second, central venous catheters are susceptible to contamination via their hubs and injection ports. These device parts are external and accessible for illumination by external sources or integrated LED source. The port and hub lumen could be regularly filled with a phenylene ethynylene antimicrobial and subjected to light induced disinfection as part of a routine infection prevention program. Third, phenylene ethynylene compounds could be grafted to external medical device materials (e.g., central venous catheter hubs, ports and tubes) to incorporate surfaces that could be regularly disinfected by application of light. In addition, phenylene ethynylenes could find medical use in the area of wound care as topically applied antimicrobials and by incorporation into wound dressings. In this setting, light activation could be applied manually from external sources during dressing changes, or in a more automated fashion from an integrated dressing LED light source, to prevent contamination of the wound. Additional costs associated with the use of antimicrobial catheter treatments and associated illumination systems would be offset by prevention of the substantial costs associated with treating catheter-associated infections, as well as by improvements in patient morbidity and mortality.

References

1. Beer DDE, Stoodley P. Microbial Biofilms. Image (Rochester, NY) 1–48.
2. Mathé L, Van Dijck P. 2013. Recent insights into Candida albicans biofilm resistance mechanisms. Curr Genet 59:251–264.
3. Baillie GS, Douglas LJ. 1998. Effect of growth rate on resistance of Candida albicans biofilms to antifungal agents. Antimicrob Agents Chemother 42:1900–5.
4. Douglas LJ. 2003. Candida biofilms and their role in infection. Trends Microbiol 11:30–36.
5. Pappas HC, Sylejmani R, Graus MS, Donabedian PL, Whitten DG, Neumann K. 2016. Antifungal Properties of Cationic Phenylene Ethynylenes and Their Impact on -Glucan Exposure. Antimicrob Agents Chemother 60:4519–4529.
6. Cannon RD, Lamping E, Holmes AR, Niimi K, Baret P V., Keniya M V., Tanabe K, Niimi M, Goffeau A, Monk BC. 2009. Efflux-mediated antifungal drug resistance. Clin Microbiol Rev 22:291–321.
7. Sanguinetti M, Posteraro B, Fiori B, Ranno S, Torelli R, Fadda G. 2005. Mechanisms of Azole Resistance in Clinical Isolates of Candida glabrata Collected during a Hospital Survey of Antifungal Resistance Mechanisms of Azole Resistance in Clinical Isolates of Candida glabrata Collected during a Hospital Survey of Antifungal Re. Society 49:668–679.
8. Holmes AR, Keniya M V., Ivnitski-Steele I, Monk BC, Lamping E, Sklar LA, Cannon RD. 2012. The monoamine oxidase A inhibitor clorgyline is a broad-spectrum inhibitor of fungal ABC and MFS transporter efflux pump activities which reverses the azole resistance of Candida albicans and Candida glabrata clinical isolates. Antimicrob Agents Chemother 56:1508–1515.
9. Odds, FC;Brown, AJ;Gow N. 2003. Antifungal agents: mechanism of action. Trends Microbiol 11:272–279.
10. Nakayama H, Tanabe K, Bard M, Hodgson W, Wu S, Takemori D, Aoyama T, Kumaraswami NS, Metzler L, Takano Y, Chibana H, Niimi M. 2007. The Candida glabrata putative sterol transporter gene CgAUS1 protects cells against azoles in the presence of serum 1264–1272.